Using really a lot of Strain to reach the Short-wave end of QCLs: Issues and Limits

W. Ted Masselink

Humboldt-University, Berlin, Germany

The people doing the work:

Humboldt Uni:

- Mykhaylo Semtsiv
- Sebastian Dressler
- Mikaela Chashnikova
- Martin Wienold
- Ismail Bayrakli
- Mathias Ziegler
- Matthias Klinkmüller
- Martin Hempel
- Stephan Machulik

- Manfred Helm and coworkers (FZ Rossendorf)
- Gottfried Strasser Group (TU Wien)
- Ken Kennedy and Richard Hogg (University of Sheffield)
- Dmitry Smirnov and Georgy Fedorov (NHMFL, Tallahassee)
- Jean Léotin and coworkers (LNCMP, Toulouse)
- Heinrich-Hertz-Institut
- Paul-Drude-Institut
- Ferdinand-Braun Institut

Supported by DFG, BMBF

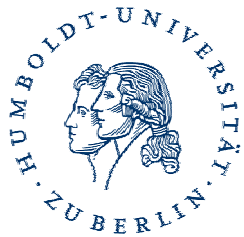

"Short wavelength QCLs" emit in 1st atmospheric window, 3–5 µm.

Gas detection:
Environmental
Medical diagnoses

Mid-IR imaging (medical)

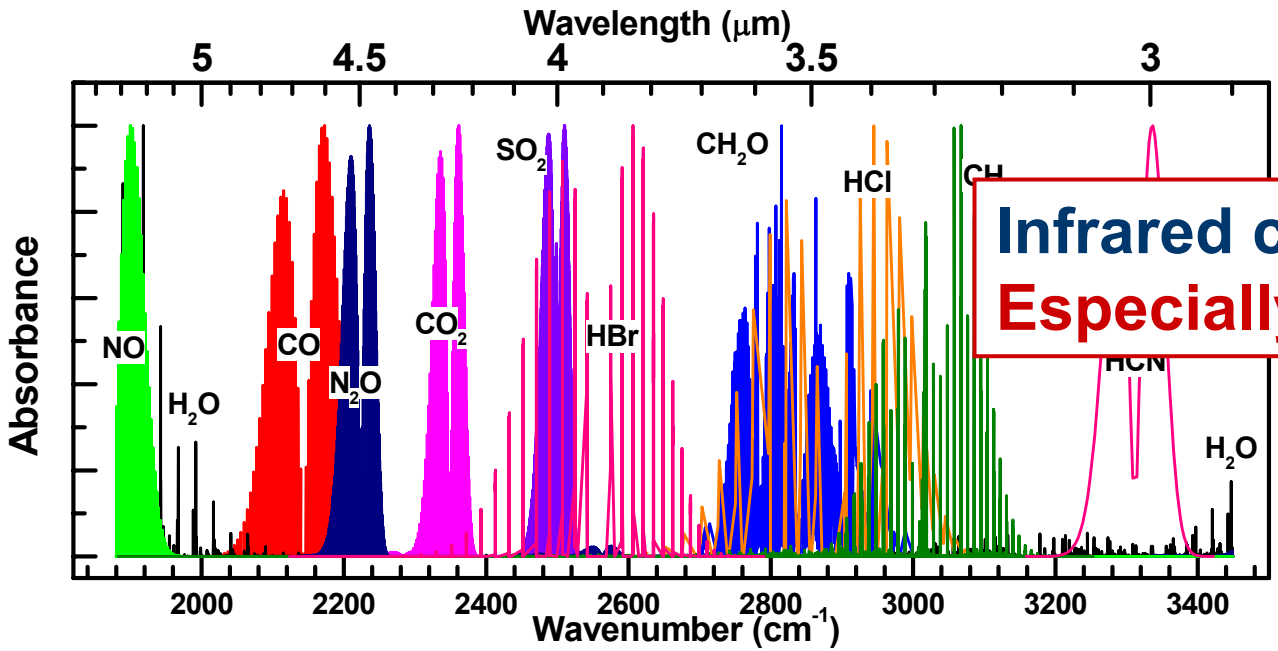

Infrared countermeasures :
Especially 3.8–4.5 µm

MIR Imaging of Squamous Cell Carcinoma

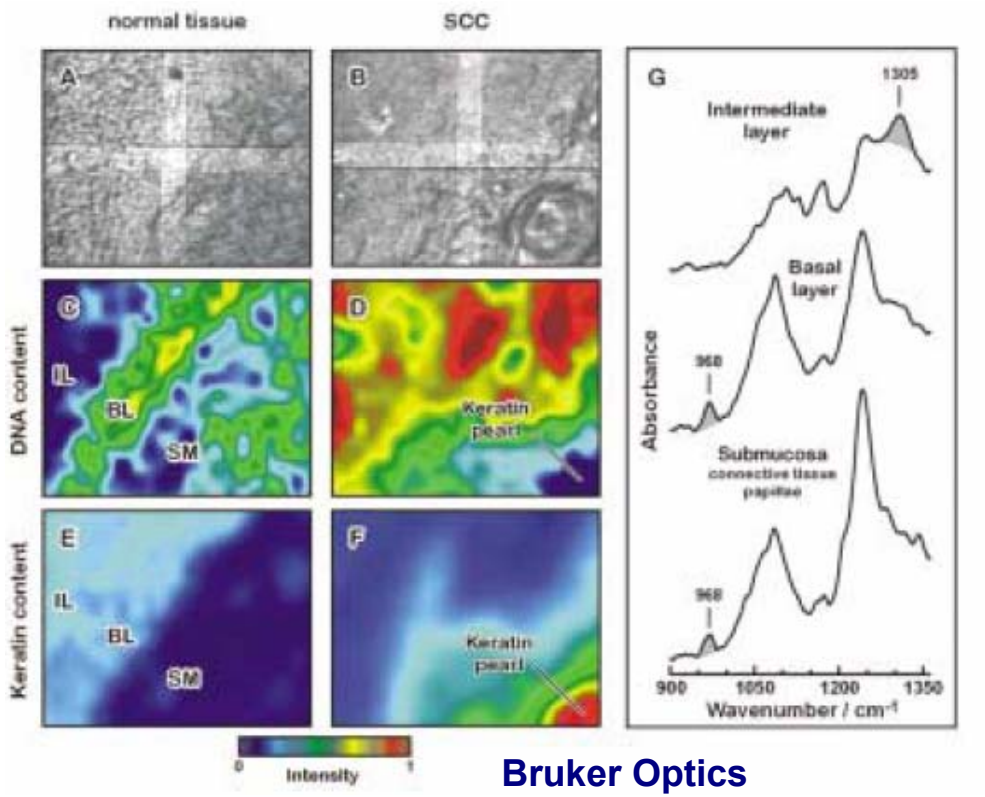

Bruker Optics

Cancerous tissue absorbs and reflects infrared light differently than does normal tissue.

HUMBOLDT-UNIVERSITÄT ZU BERLIN

Why is 3–5 μm "short wavelength" for QCLs?

- 3–5 μm ⇒ 250–410 meV
- Even for longer wavelength QCLs, you can't get photon energies greater than ½ of the difference in conduction band edge ⇒ $\Delta E_c \approx$ 500–800 meV

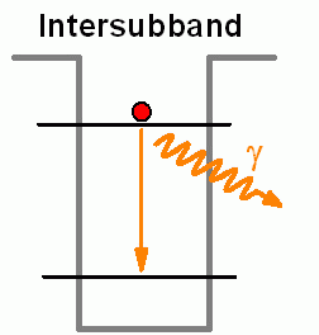

- For GaAs/AlGaAs, $\Delta E_c \approx$ 350 meV
- For (Ga,In)As / (Al,In)As lattice-matched to InP, $\Delta E_c \approx$ 530 meV

Semiconductor-based lasers for 3–5 µm:

Use both conduction and valence bands:

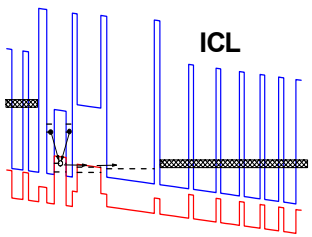

Type-II GaSb-based ICL

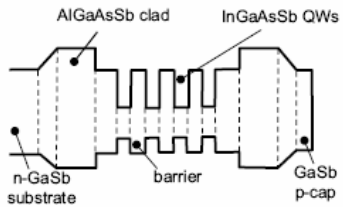

Type-I GaSb-based p-n diode lasers

Semiconductor-based lasers for 3–5 µm:

Use only the conduction band, but with large ΔE_c:

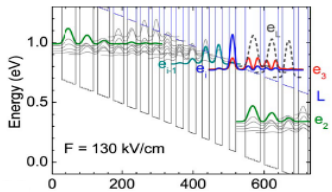

InAs/AlSb QCLs

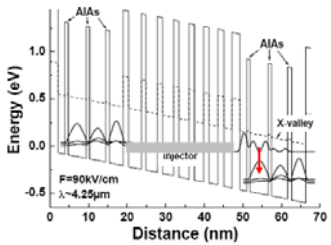

InGaAs/AlAsSb QCLs

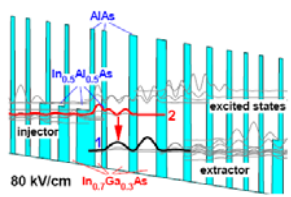

Strain-compensated InP-based QCLs

Adding strain to increase performance is not a new idea:

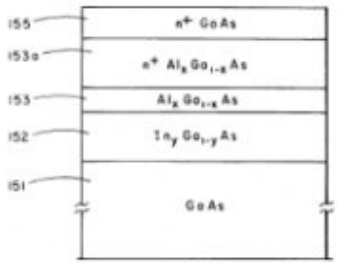

Fig. 1

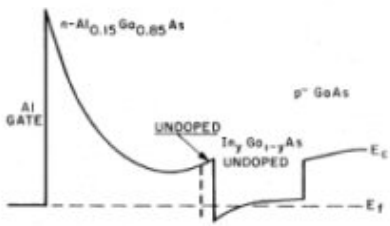

Fig. 2

pHEMT:

U.S. Patent 4,827,320 "Semiconductor with Strained InGaAs Layer“ (1989)

“Transistor Performance and Electron Transport Properties of High Performance InAs Quantum-Well FET's", IEEE EDL (1994).

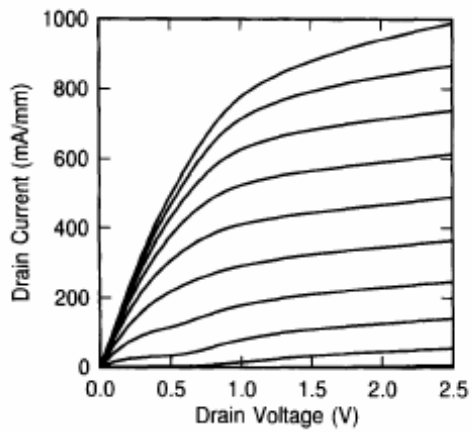

Fig. 2. FET characteristics for a 0.5-μm gate length transistor. The sample has a 300-Å uniformly doped channel with 30 Å of InAs inserted. Gate voltage increments are in -0.2 V; the top curve corresponds to $V_g = 0.4$ V.

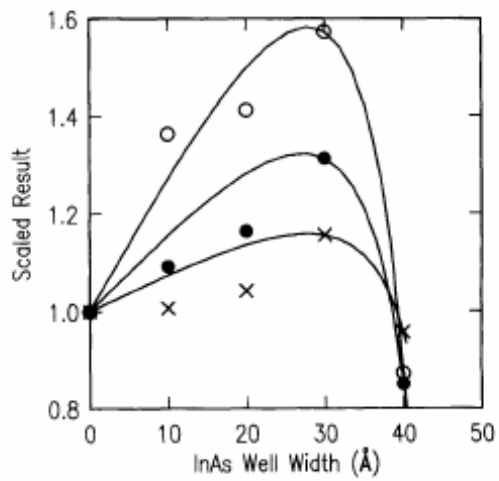

Fig. 3. Dependence of low-field mobility (•), peak electron velocity (×), and 1.8-μm transistor transconductance (○) on InAs quantum well thickness.

Strain compensation is also not new in QCLs:

APPLIED PHYSICS LETTERS VOLUME 72, NUMBER 6 9 FEBRUARY 1998

Short wavelength ($\lambda \sim 3.4\ \mu m$) quantum cascade laser based on strained compensated InGaAs/AlInAs

Jérôme Faist,[a] Federico Capasso,[b] Deborah L. Sivco, Albert L. Hutchinson, Sung-Nee G. Chu, and Alfred Y. Cho
Bell Laboratories, Lucent Technologies, Murray Hill, New Jersey 07974

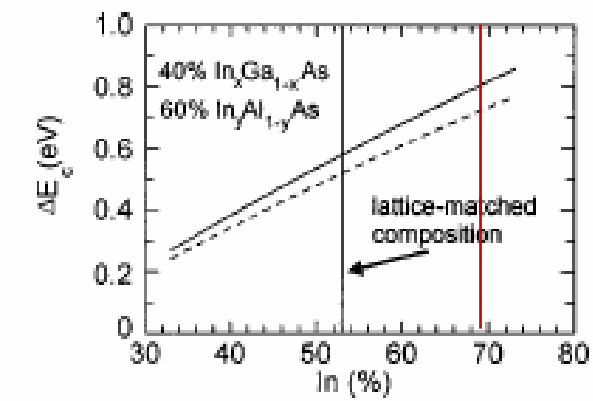

⇒λ=3.49 µm

We expect at least 5 advantages from strain compensated structures on InP:

Ranked by importance:

1. Larger ΔE_c than without strain to achieve a larger transition energy between the ULL and LLL.
2. Strain increases the energetic separation between the Γ valley and the X and L valleys.
3. AlAs blocks the leakage of the ULL into the upper states of the extractor/injector miniband.
4. Strain compensation allows using (Al,In)As as the “well material” for the ULL.
5. Strain compensation allows the use of InAs for the LLL.

We’ll look at each of these in the next foils.

We can greatly increase ΔE_c through compensated strain.

Maximize ΔE_c in the (In,Al)As/(In,Ga)As system using AlAs and $In_{0.7}Ga_{0.3}As$ (strain-compensated).

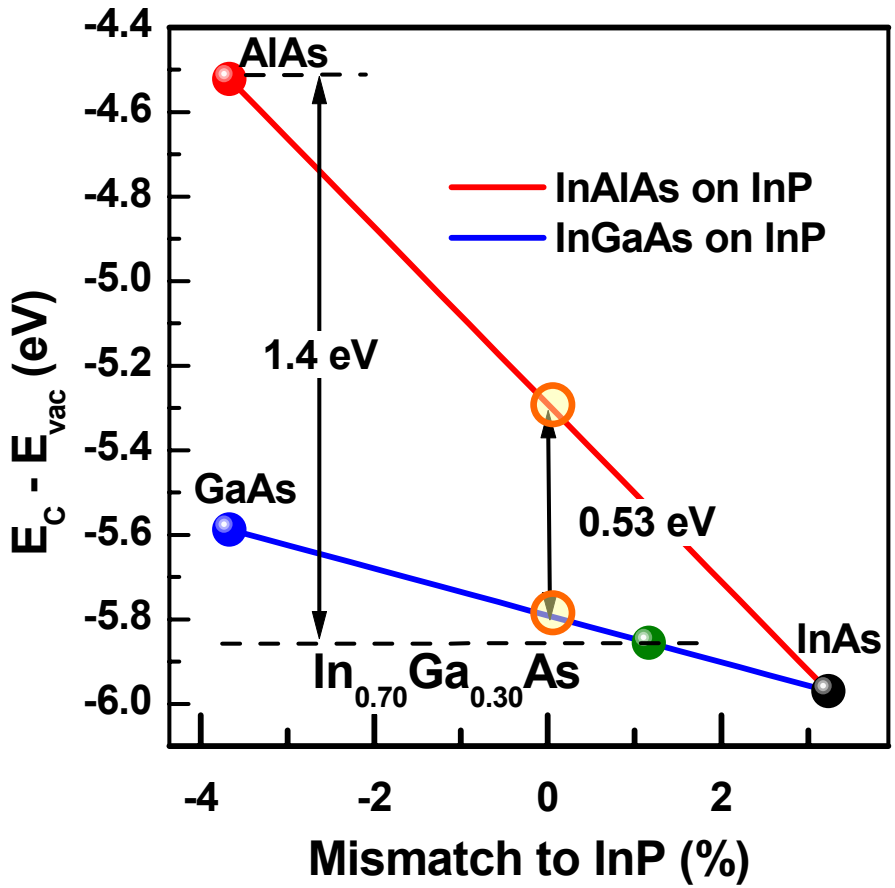

The strain partially works against a large ΔE_c.

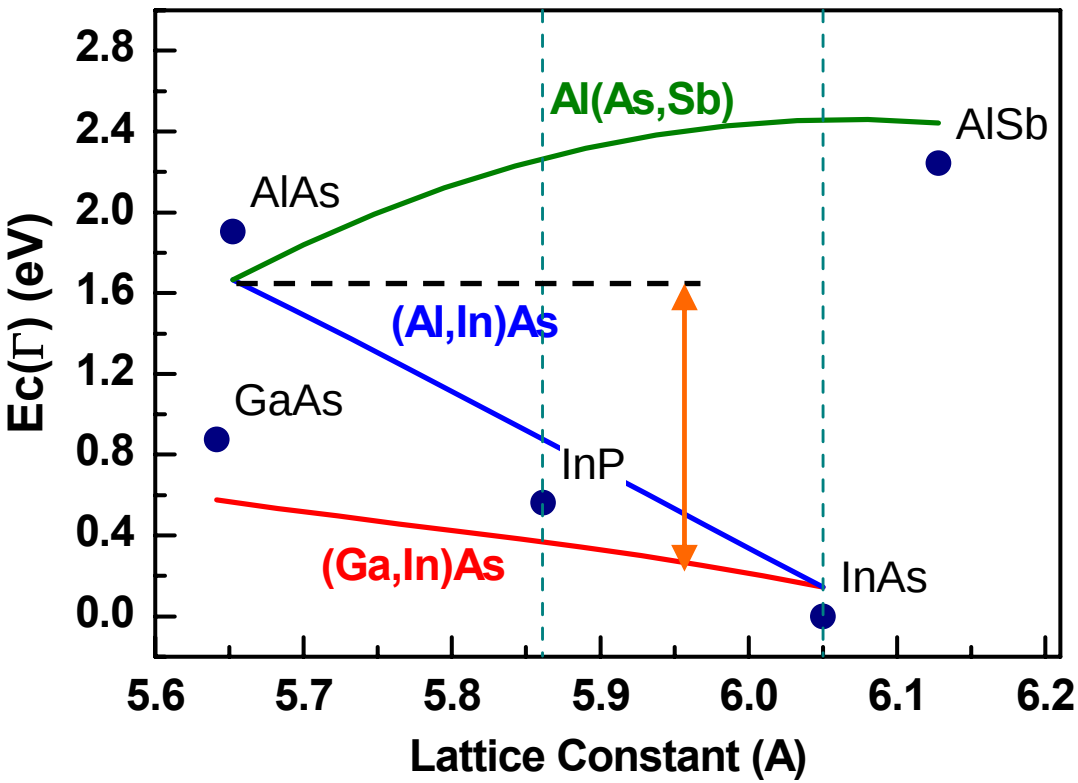

Compressively strained InAs has $E_c \approx 160$ meV higher than unstrained.

Tensilely strained AlAs has $E_c \approx 240$ meV lower than unstrained.

(Ga,In)As-AlAs
$\Delta E_c \approx 1.5$ eV

We can compare the ΔE_c in several direct-band-gap III-V heterosystems.

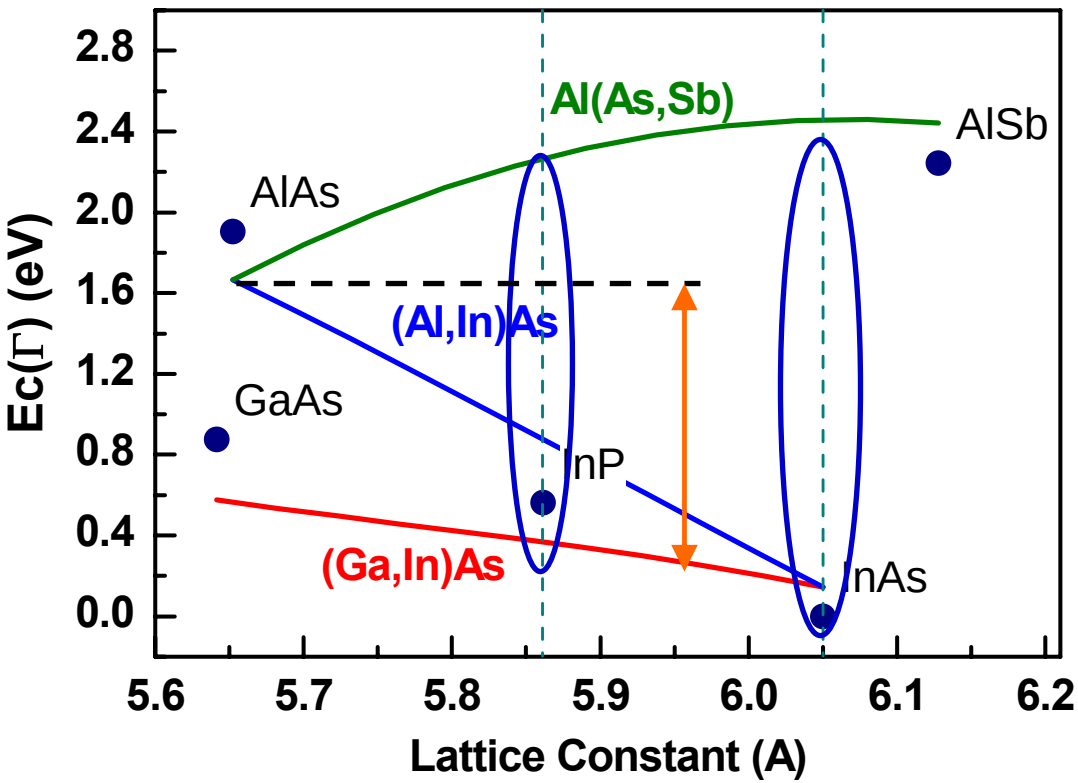

(Ga,In)As-AlAs
$\Delta E_c \approx 1.5$ eV

(Ga,In)As-Al(As,Sb)
$\Delta E_c \approx 1.6$ eV

InAs-Al(As,Sb)
$\Delta E_c \approx 2.1$ eV

The internal strains are large:

- For AlAs on InP, $\varepsilon_{||}$ is about +3.7%
- For $In_{0.7}Ga_{0.3}As$ on InP, $\varepsilon_{||}$ is about -1.6%
- For InAs on InP, $\varepsilon_{||}$ is about -3.5%

With higher growth temperatures, the compressive strain drives the formation of quantum dots or wires.

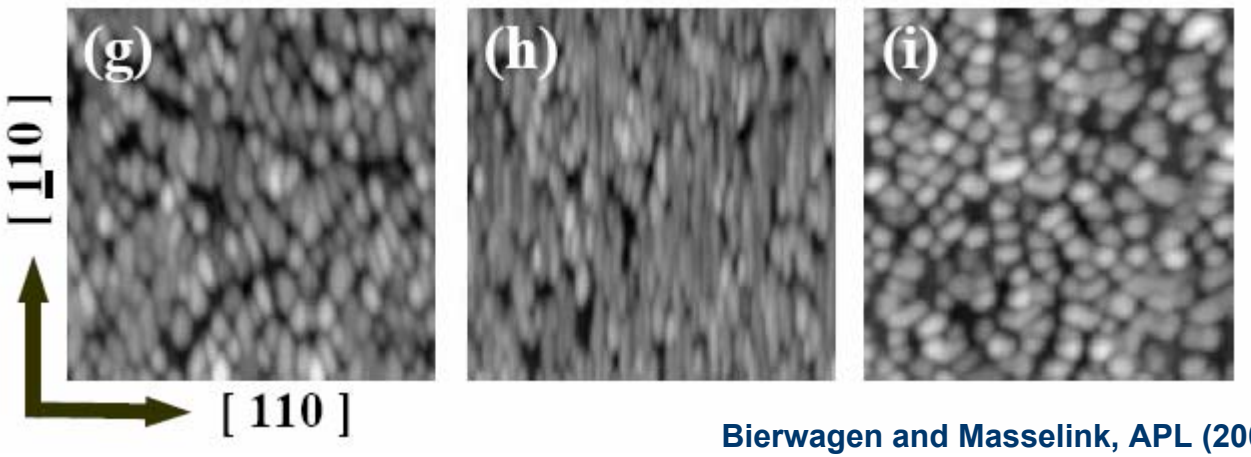

Bierwagen and Masselink, APL (2005).

Structures are grown using gas-source MBE for excellent InP

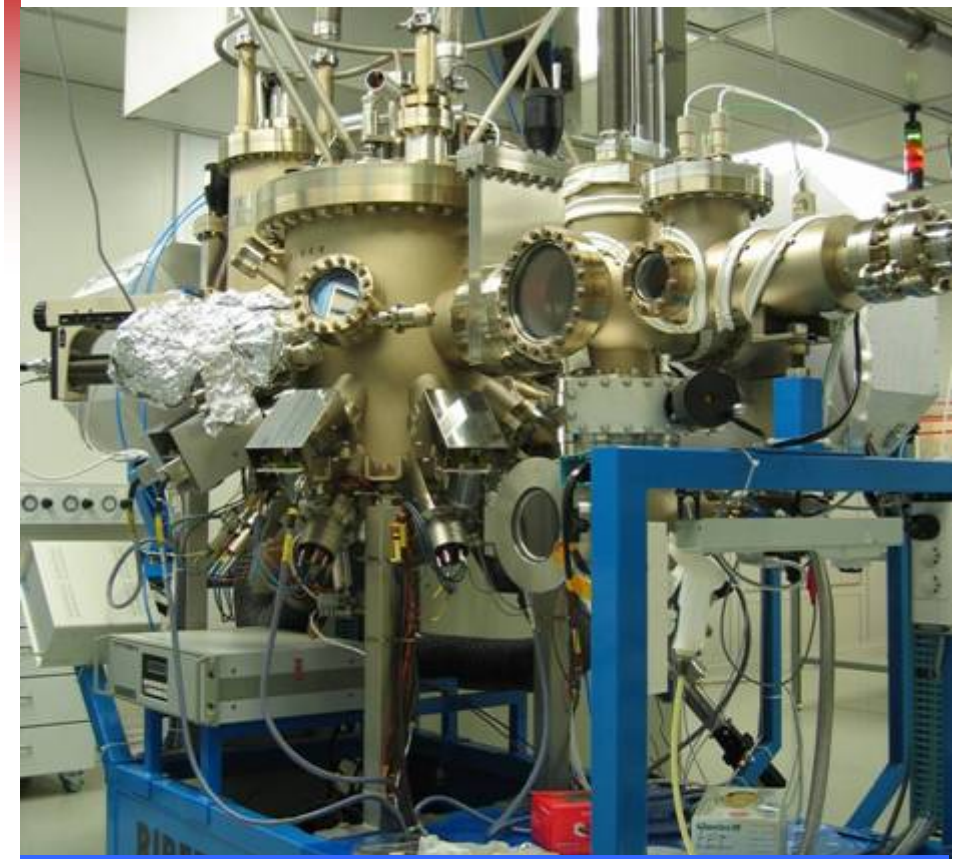

Riber Compact 21T

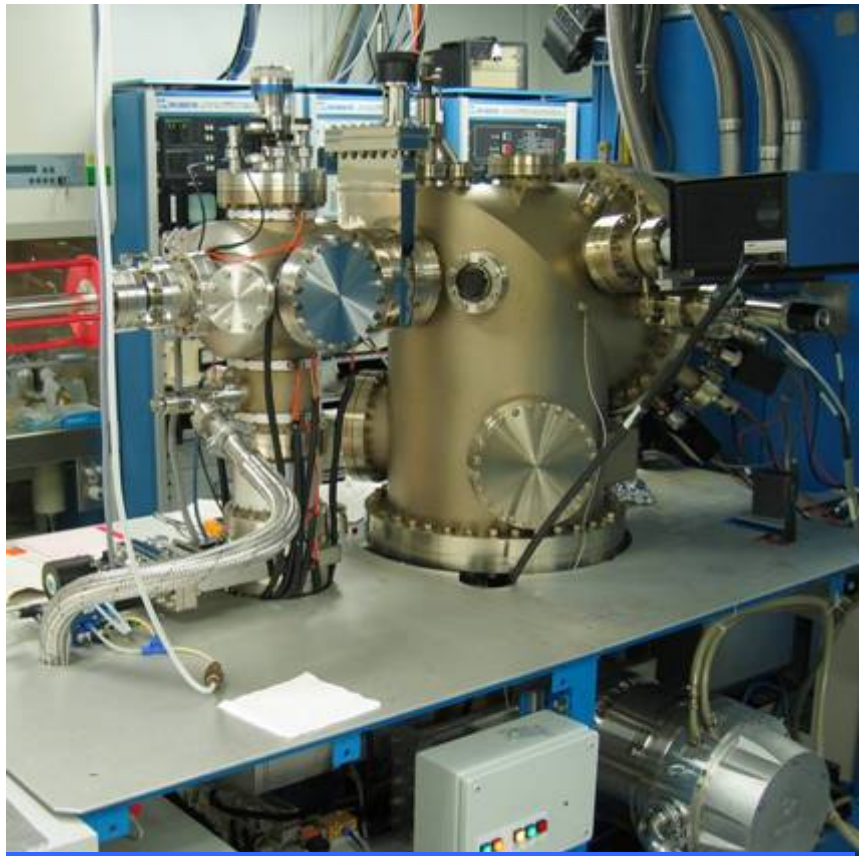

Riber 32P GSMBE

Handling Hydrides

- Liquid hydride sources
- Delivery < 1 bar
- Mass-flow or pressure controlled
- Run-vent
- Cracked inlet @ 850 °C
- Detector system, fully interlocked
- All cabinets at underpressure; gas lines encapsulated

Strain compensation has open questions.

To achieve strain compensation, we usually require that the in-plane lattice constant of the system matches the substrate:

$$a_{InP} = \frac{a_B h_B + a_W h_W}{h_B + h_W}$$

Or, $\frac{h_B}{h_W} = -\frac{\Delta a_W}{\Delta a_B}$ **For AlAs/In$_{0.7}$Ga$_{0.3}$As,** $\frac{h_B}{h_W} \approx 0.4$

If we include the differences in shear moduli, $\frac{h_B}{h_W} = -\frac{\Delta a_W}{\Delta a_B}\frac{G_W^{001}}{G_B^{001}}$

Then, for AlAs/In$_{0.7}$Ga$_{0.3}$As, $\frac{h_B}{h_W} \approx 0.3$

Vegard's Law ⇒ for thin layers, the material is characterized by a single shear modulus.

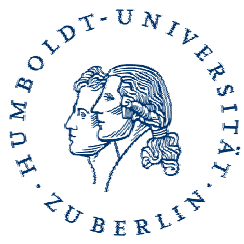

Global strain is compensated; also important to avoid excessive local strain

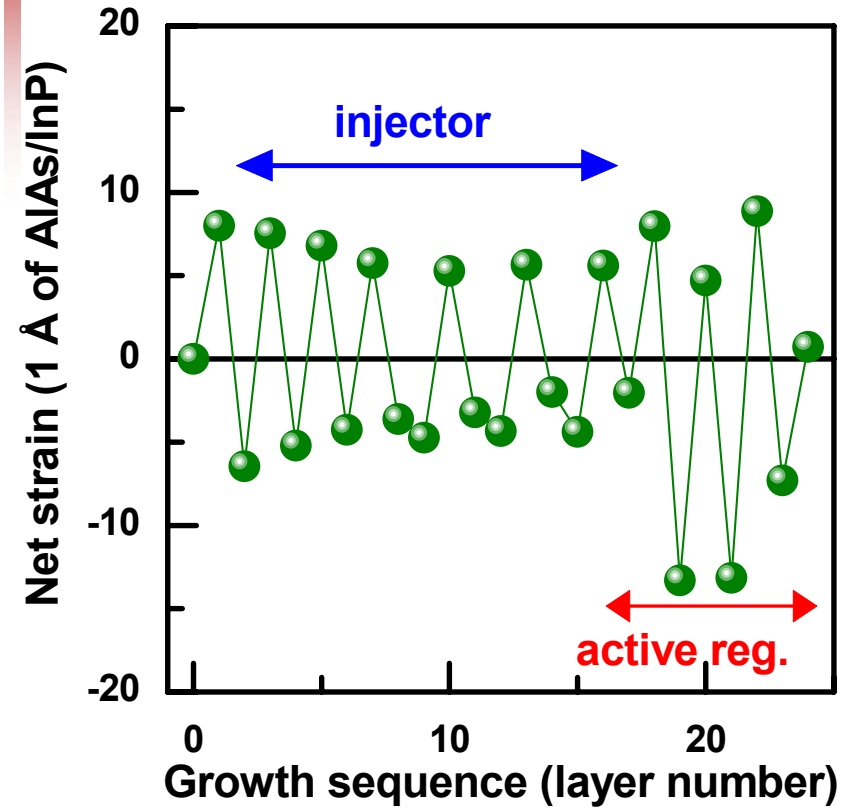

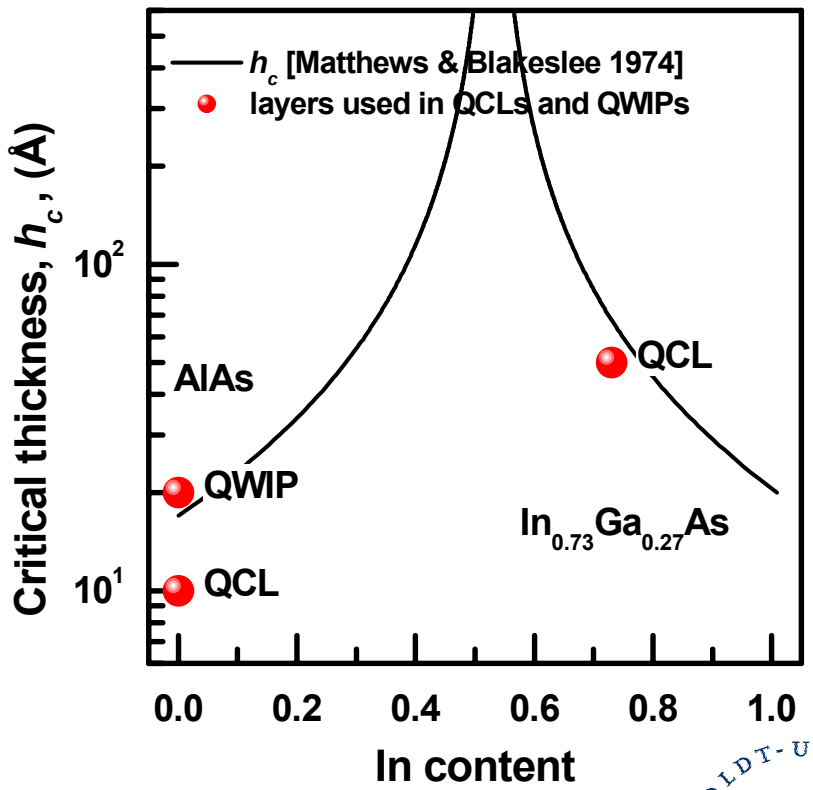

The average valence band edge is calculated relative to the vacuum level.

Van de Walle (1989) tabulates the valence band energy (without spin) on an absolute scale.

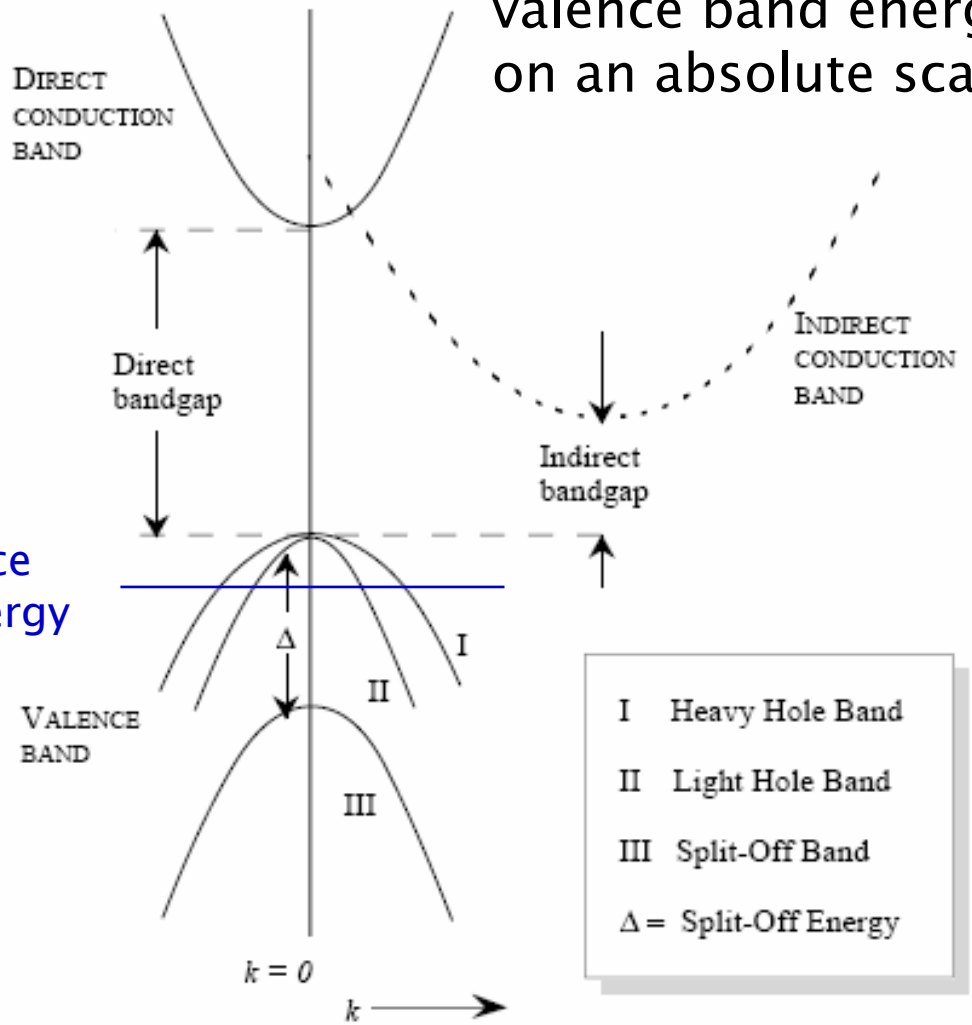

Spin is added in "by hand" and adding E_g gives the conduction band edge.

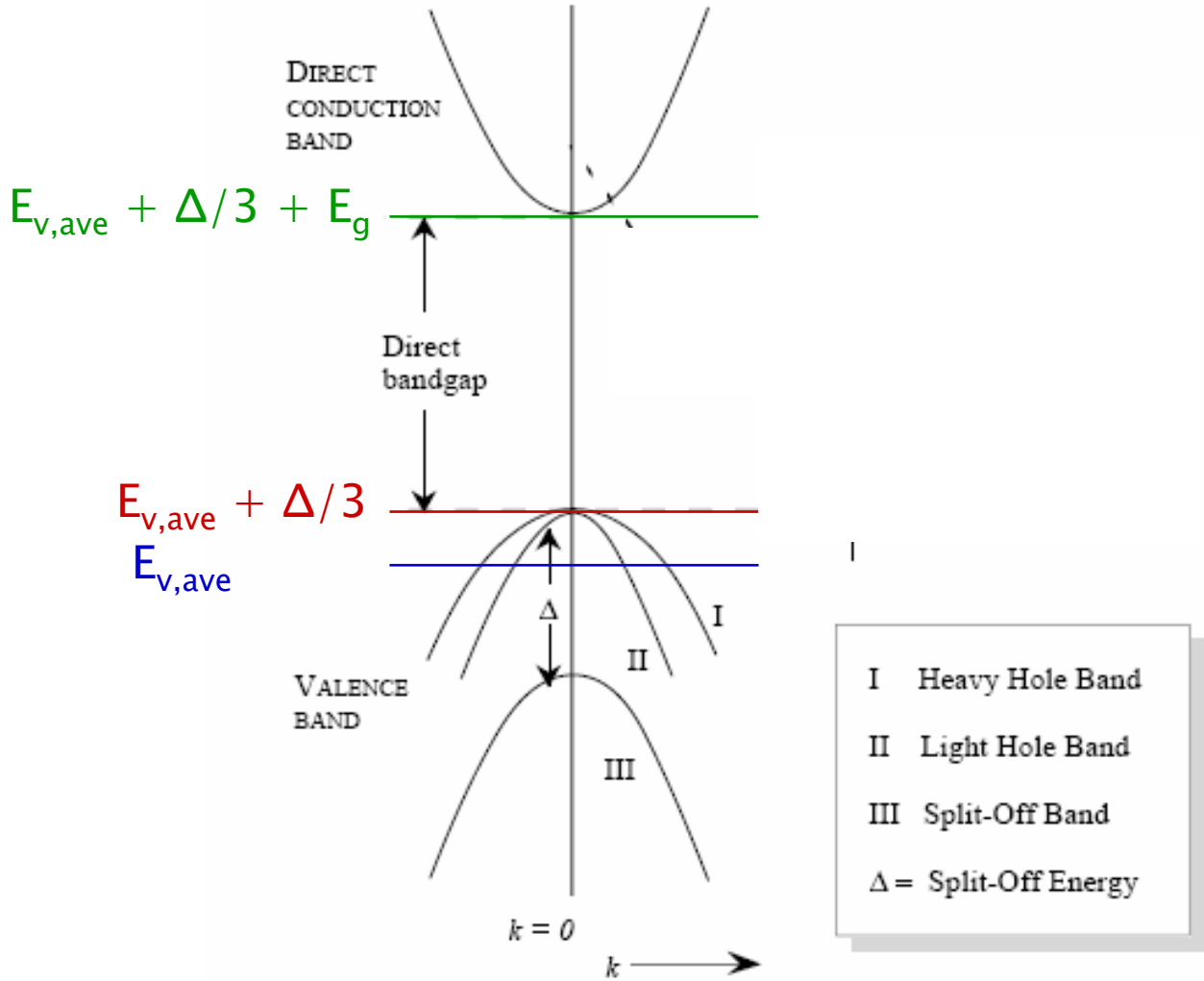

The conduction band is distorted due to strain: each valley through its deformation potential.

$$\Delta E_c = a_c \frac{\Delta\Omega}{\Omega}$$

(deformation potential × relative change in volume)

For the Γ valley, only the hydrostatic strain results in a change.

$$\frac{\Delta\Omega}{\Omega} = \varepsilon_{xx} + \varepsilon_{yy} + \varepsilon_{zz} = 2\varepsilon_{\parallel} + \varepsilon_{\perp}$$

$$= (2 - D^{001})\varepsilon_{\parallel}$$

$$\varepsilon_{\parallel} = \frac{a_{InP}}{a_i} - 1$$

The biaxial strain component further splits the X valleys

$$\Delta E_X = \Xi^{\Delta}(\varepsilon_{\perp} - \varepsilon_{\parallel}) = -\Xi^{\Delta}(1 + D^{001})\varepsilon_{\parallel}$$

For $In_{0.7}Ga_{0.3}As$,

$$\varepsilon_{\parallel} \approx -0.016$$

$$(1 + D^{001}) \approx 2$$

$$\Xi^{\Delta} \approx 5 \text{ eV}$$

$$\Delta E_X \approx 160 \text{ meV}$$

The lower X valleys are the transverse valleys, so they are about 50 meV lower than the X position calculated from hydrostatic strain.

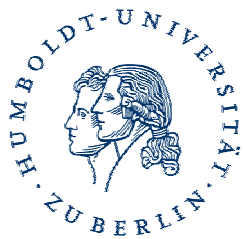

The AlAs/$In_{0.73}Ga_{0.27}As$ system allows high-energy intersubband transitions

We expect maybe 0.75 eV (1.7 μm)

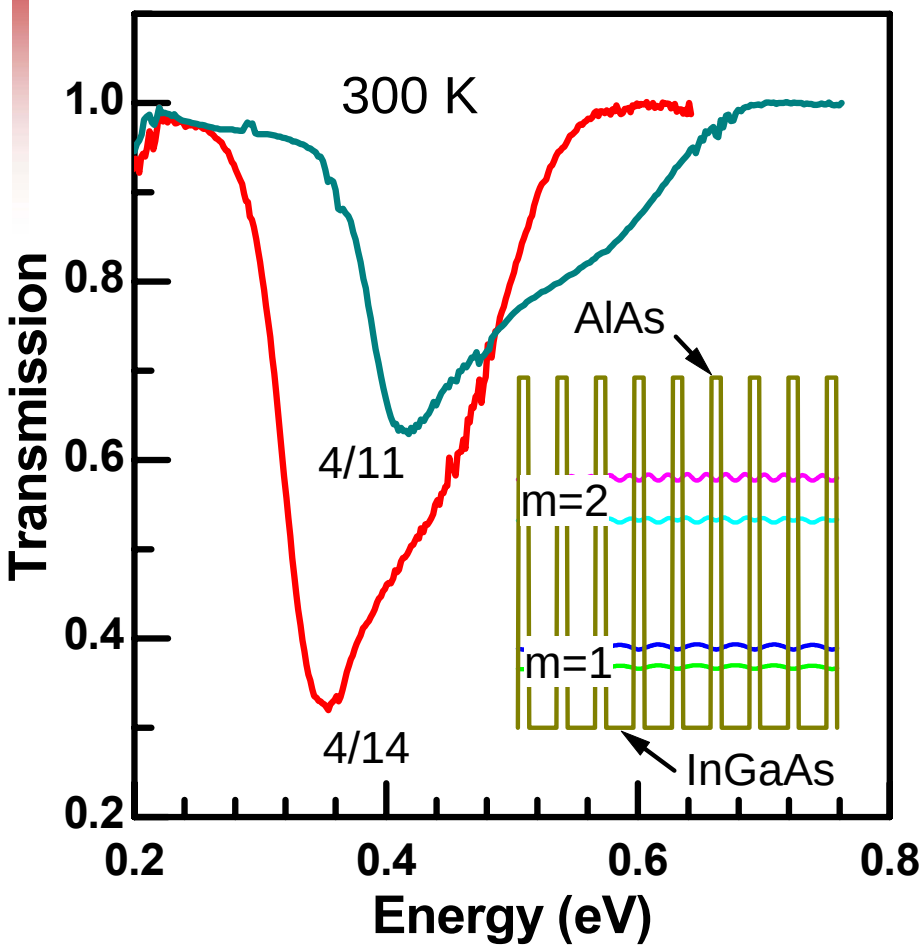

AlAs: 1.2 nm

$In_{0.73}Ga_{0.27}As$: 4.2 and 3.3 nm

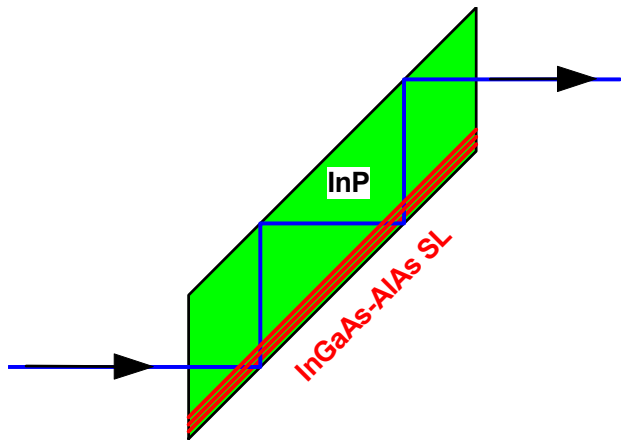

4.2 nm ⇒ 0.35 – 0.43 eV

3.3 nm ⇒ 0.42 – 0.55 eV

⇒ 2.3 μm

Georgiev, et al. APL, 2003.

Strain compensation is an additional constraint on design.

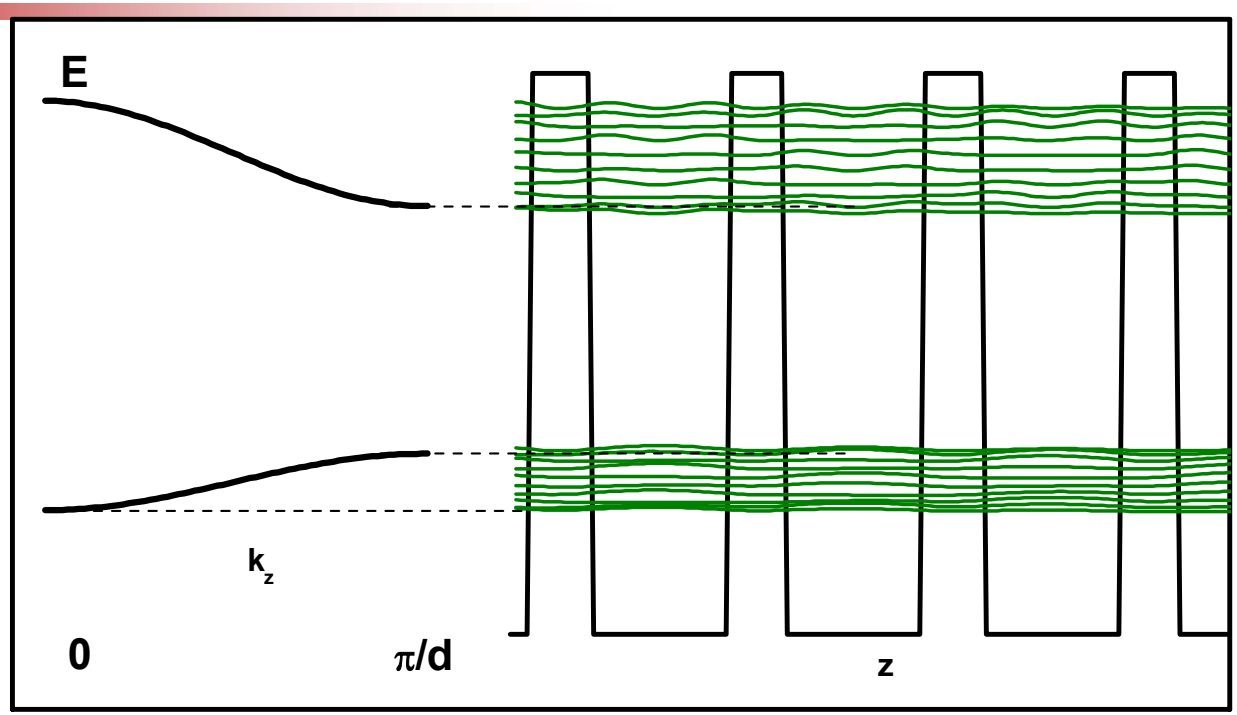

Narrower minibands would need thicker AlAs, but with thin InGaAs…

Composite Barriers based on AlAs ⇒ independent control of energy and strain

Replace the AlAs with $In_{0.55}Al_{0.45}As$ + AlAs

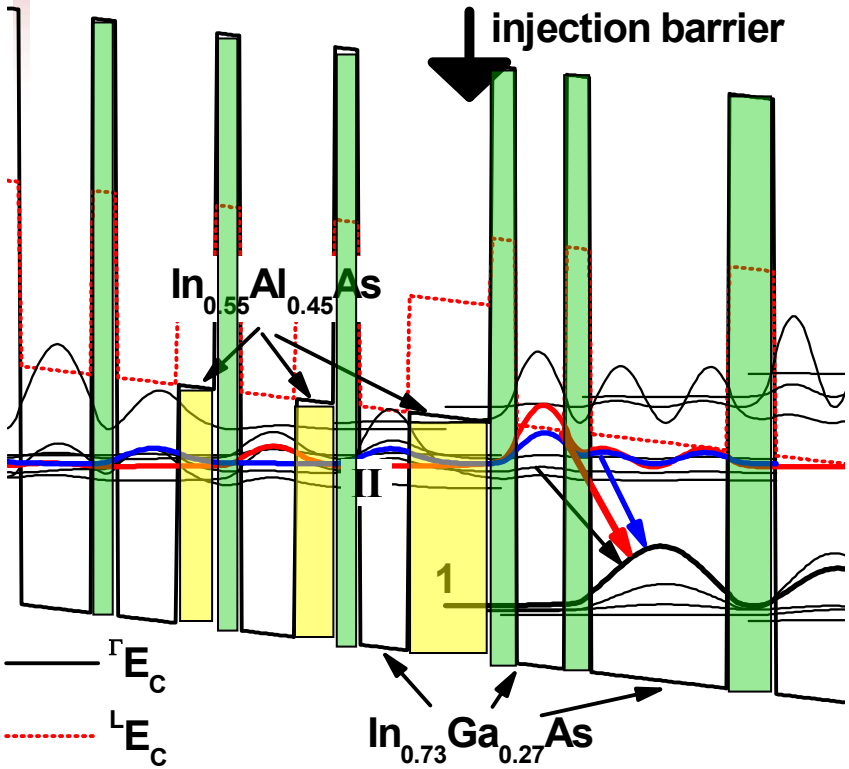

Addition of $In_{0.55}Al_{0.45}As$

- **shrinks miniband**
- **partially compensates for thicker AlAs**
- **independent control of confinement and strain**

Can also use AlAs with addition of Al(As,Sb).

Using composite barriers of AlAs + $In_{0.55}Al_{0.45}As$, the miniband is shrunk and absorption energies are high.

We now expect closer to 0.75 eV (1.7 μm)

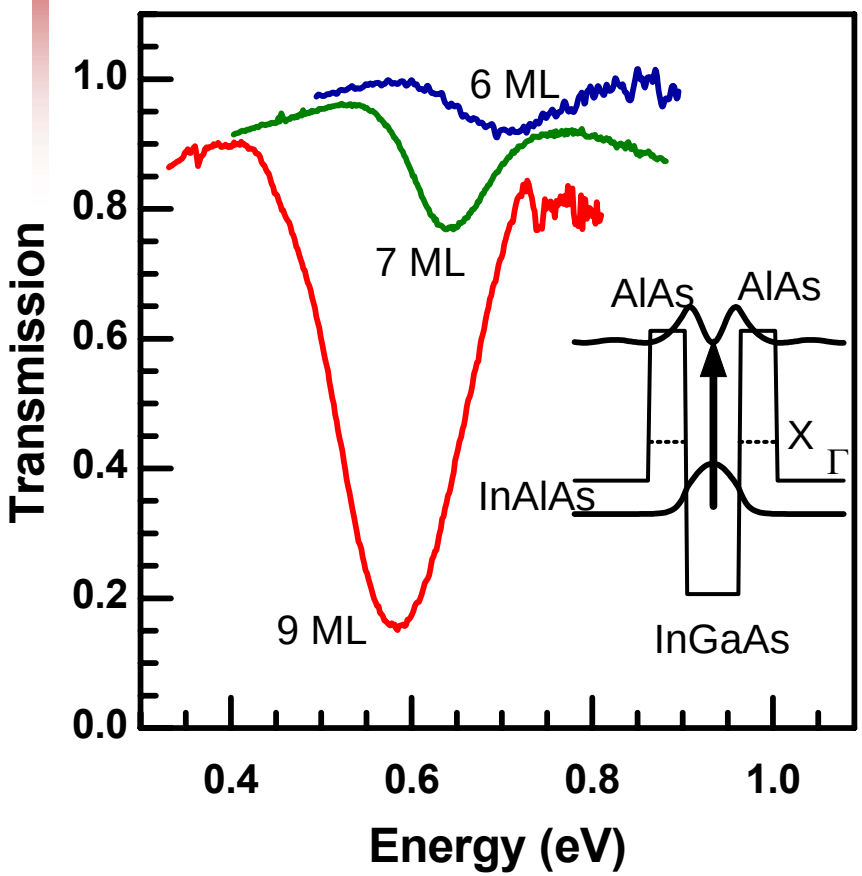

AlAs: 1.5 or 2.0 nm
InGaAs: 2.8, 2.2, 1.9 nm

2.8 nm ⇒ 0.58 eV, 2.14 μm
2.2 nm ⇒ 0.66 eV, 1.88 μm
1.9 nm ⇒ 0.72 eV, 1.72 μm

No dispersion thanks to thicker composite barriers; broadening due to non-parabolicity with high doping.

Semtsiv, et al. JAP, 2005.

In QCL, most barriers are AlAs, with composite barriers used for better confinement.

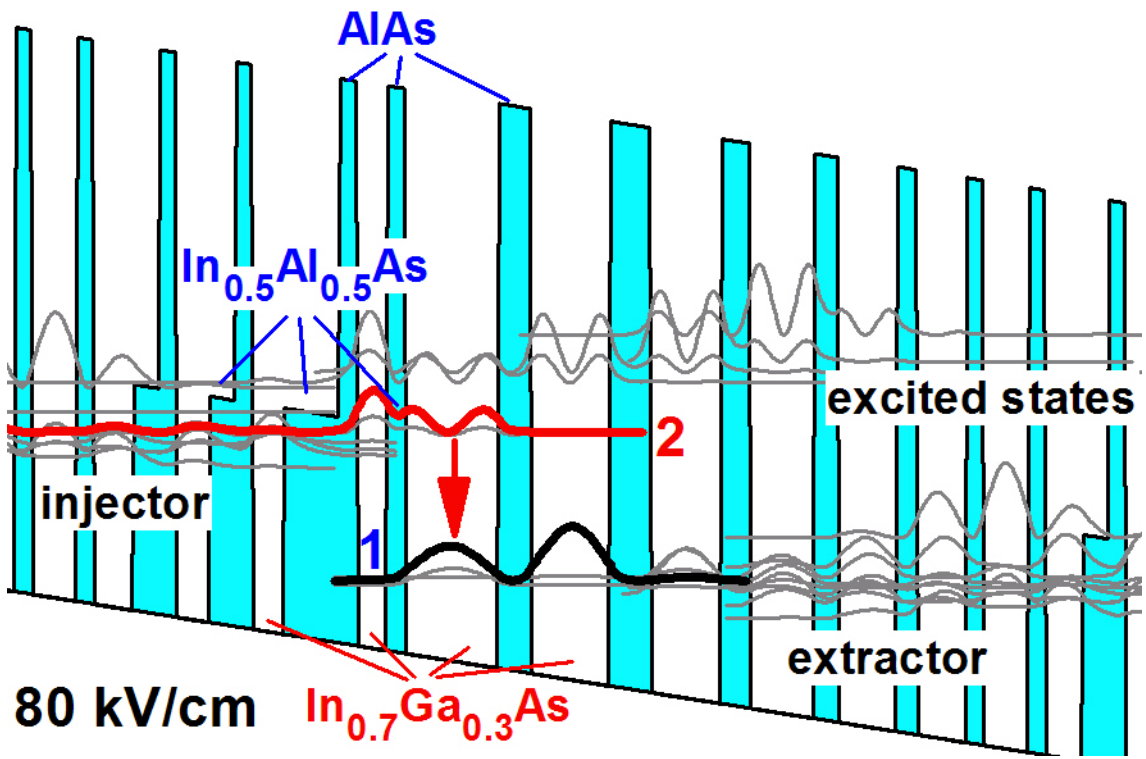

The design uses the transition from a few upper states into a single lower state that is connected to a miniband.

AlAs also prevents unwanted tunneling out of the upper laser level.

For small barriers, AlAs can help prevent tunneling out of the upper laser level into the continuum.

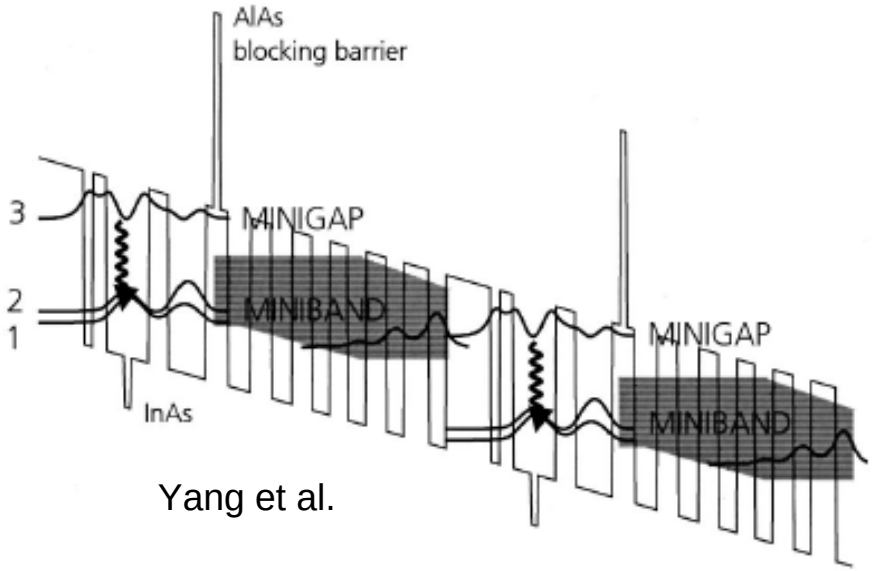

Yang et al.

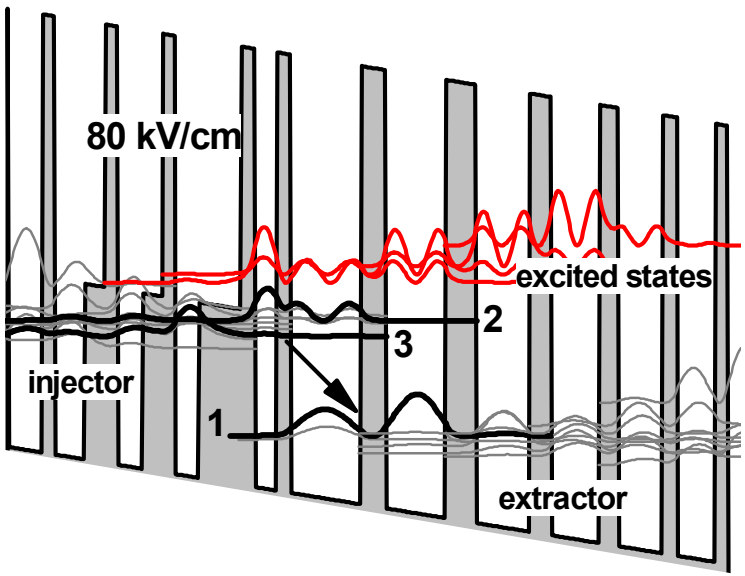

In our case, there is also an upper miniband we need to avoid.

The emission wavelength is limited by the indirect valleys in the well, not by ΔE_c.

E_2 is limited by the indirect valleys in the InGaAs wells.

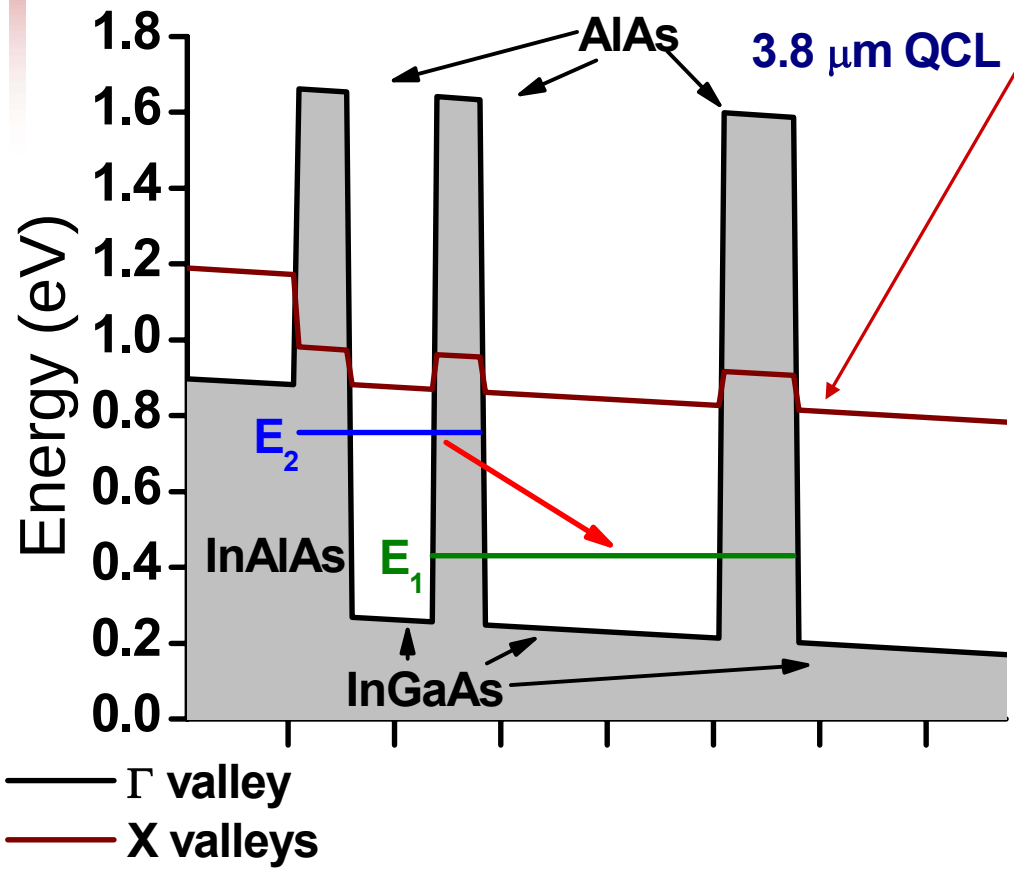

Questions:

Where is the next state above E_2?

How to maximize E_2–E_1 keeping E_2 away from the indirect valleys?

Optimize well material for large indirect-Γ energy separation, moderate strain.

The indirect-Γ separation increases with In content. The maximum transition energy increases correspondingly.

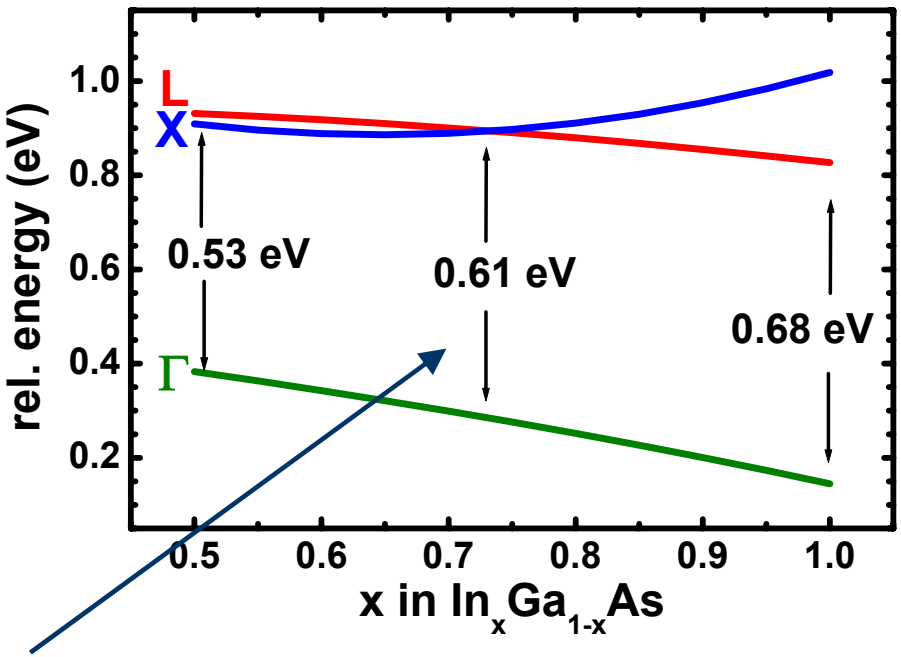

$0.53\text{eV} \Rightarrow \lambda_{min} \approx 3.8\ \mu\text{m}$
$0.61\text{eV} \Rightarrow \lambda_{min} \approx 3.3\ \mu\text{m}$
$0.68\text{eV} \Rightarrow \lambda_{min} \approx 2.9\ \mu\text{m}$

For relaxed InAs, $\lambda_{min} \approx 2.7\ \mu\text{m}$.

$In_xGa_{1-x}As$ with $x \approx 0.72$

The poor coupling between Γ and X should help us, though.

Relaxation from Γ_2 directly to Γ_1 is 4 times faster than via the X valleys.

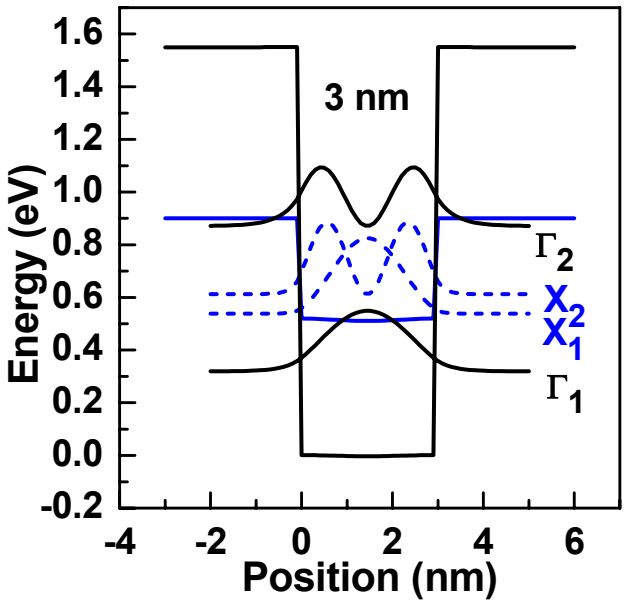

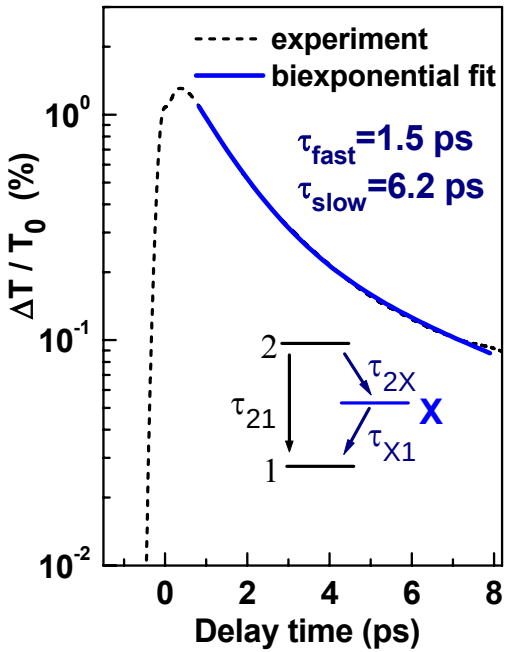

So we should be able to put Γ_2 > X.

How far?
How best?

(Courtesy H. Schneider, Forschungszentrum Dresden Rossendorf, Germany)

Designs for 3.8 µm and 3.6 µm

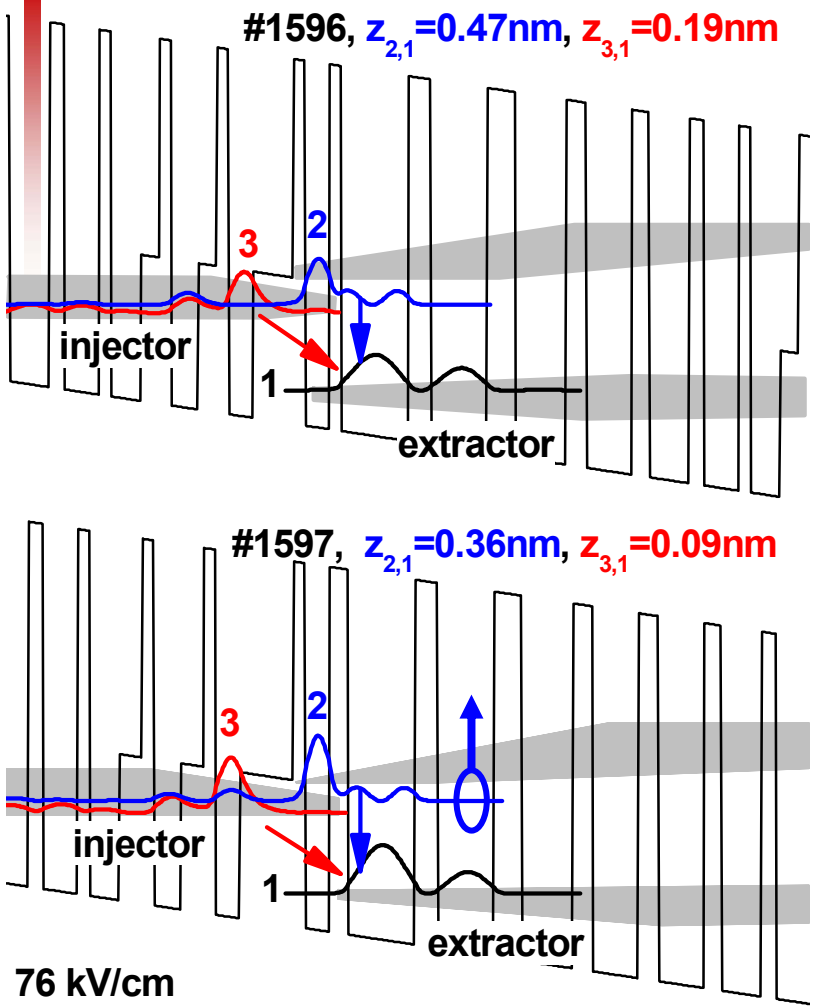

1596: for 3.8 µm

1597: for 3.6 µm

Both designs are similar, but 1597 has a thicker AlAs barrier to the left of the main QW to lift state 2 without lifting state 1. Thus, E_{21} increases.

1596 and 1597: Both lase at 3.8 μm

We see several differences between 1596 (3.8 μm) and 1597 (3.6 μm): 1596 has broader EL and a lower threshold current.

But, both lase at 3.8 μm.

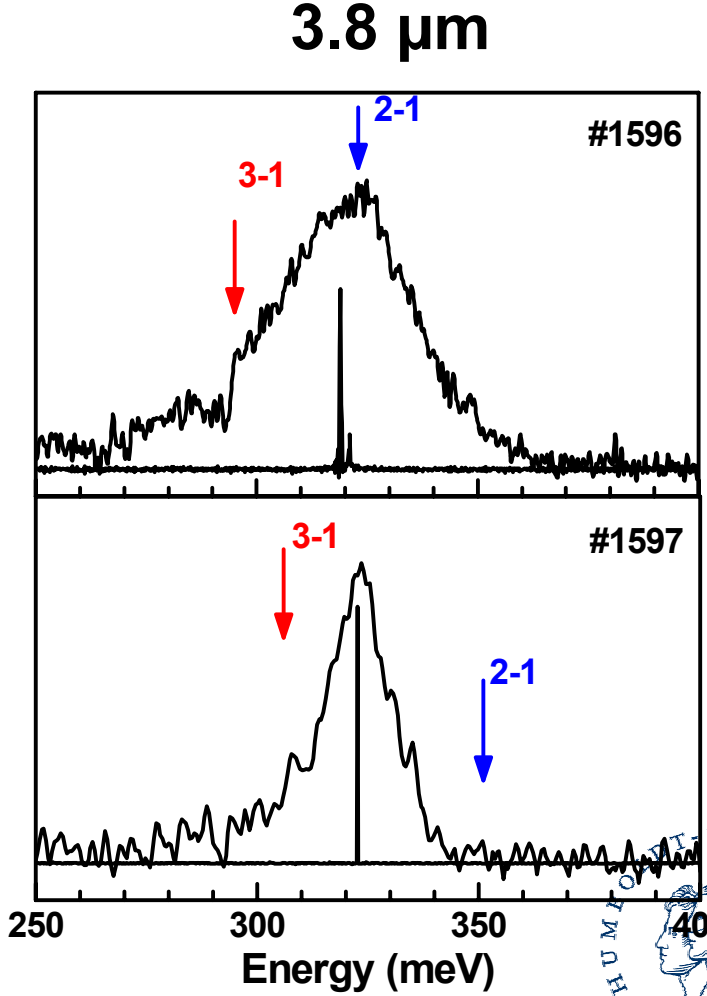

Take the Lasers to Tallahassee

Resistive magnet up to 33 T.

Advantage over pulsed magnet is for measuring laser spectrum as function of B.

(with D. Smirnov and G. Federov)

Experimental Observations

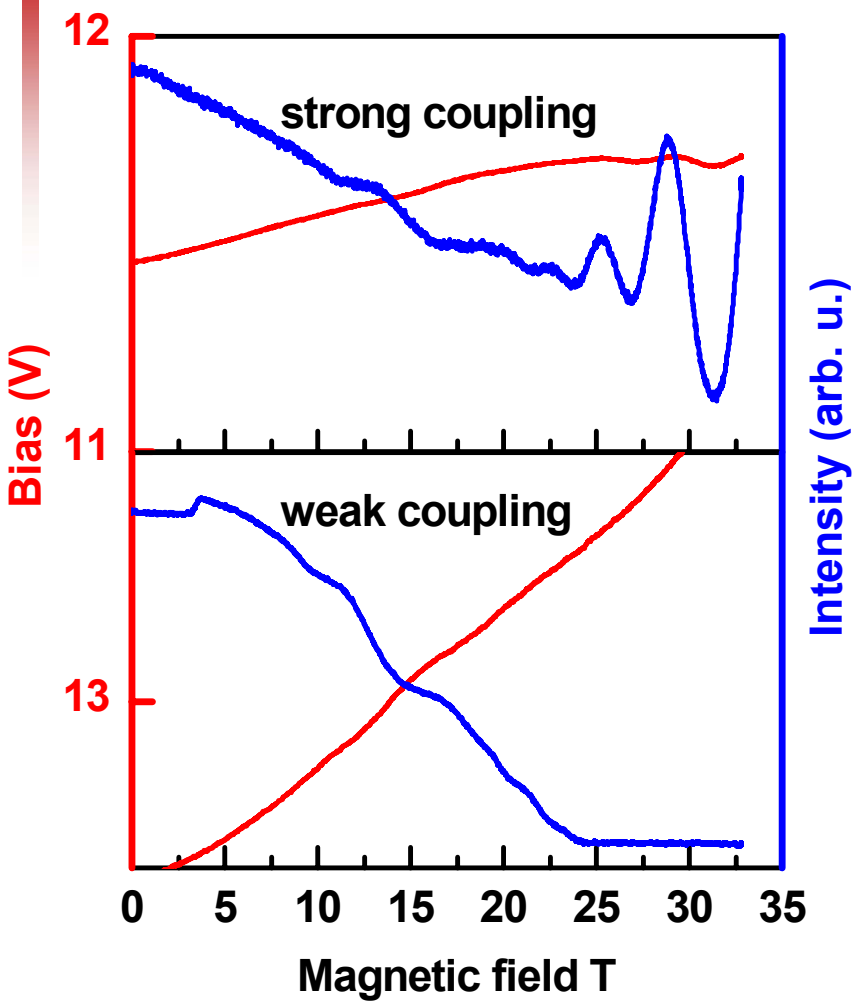

Conditions are T=6K, constant current during 100-ns current pulse.

1. Emission intensity oscillates with B field.
2. Bias voltage required to maintain current increases with B and oscillates with emission.

Experimental Observations

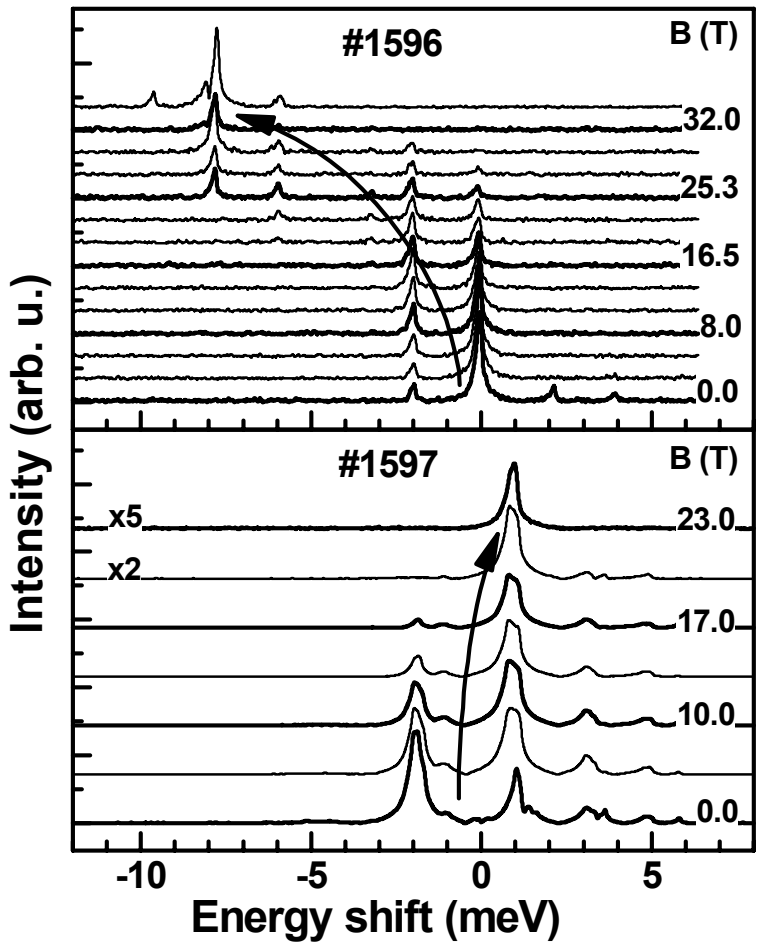

3. Wavelength shift in emission spectrum: red shift for 1596, blue shift for 1597.

Energy shift with B-field for N=0 Landau Levels

The lasing action takes place between the N=0 Landau levels of the i=2 and 1 states.

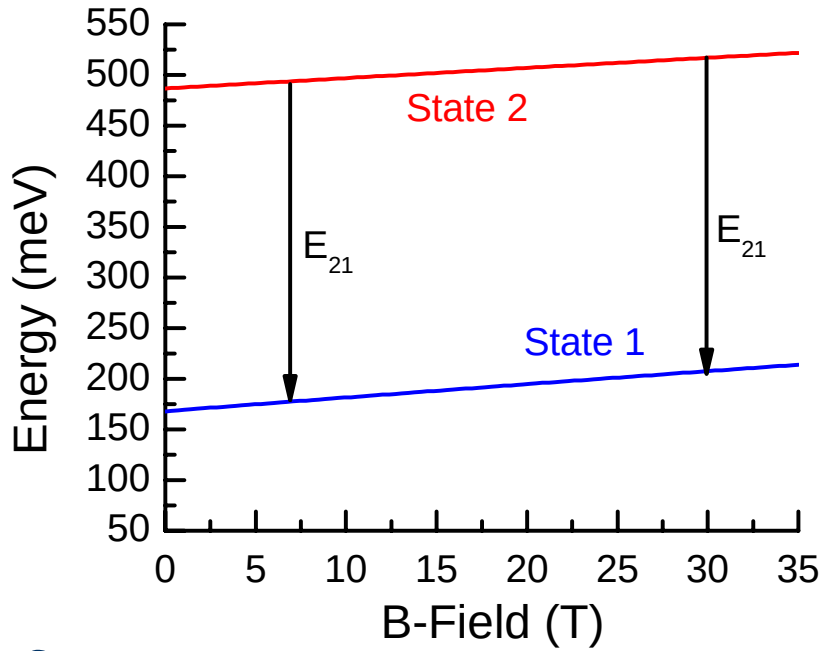

E_2-E_1 **is almost independent of** B.

Why is light emission reduced for specific values of B?

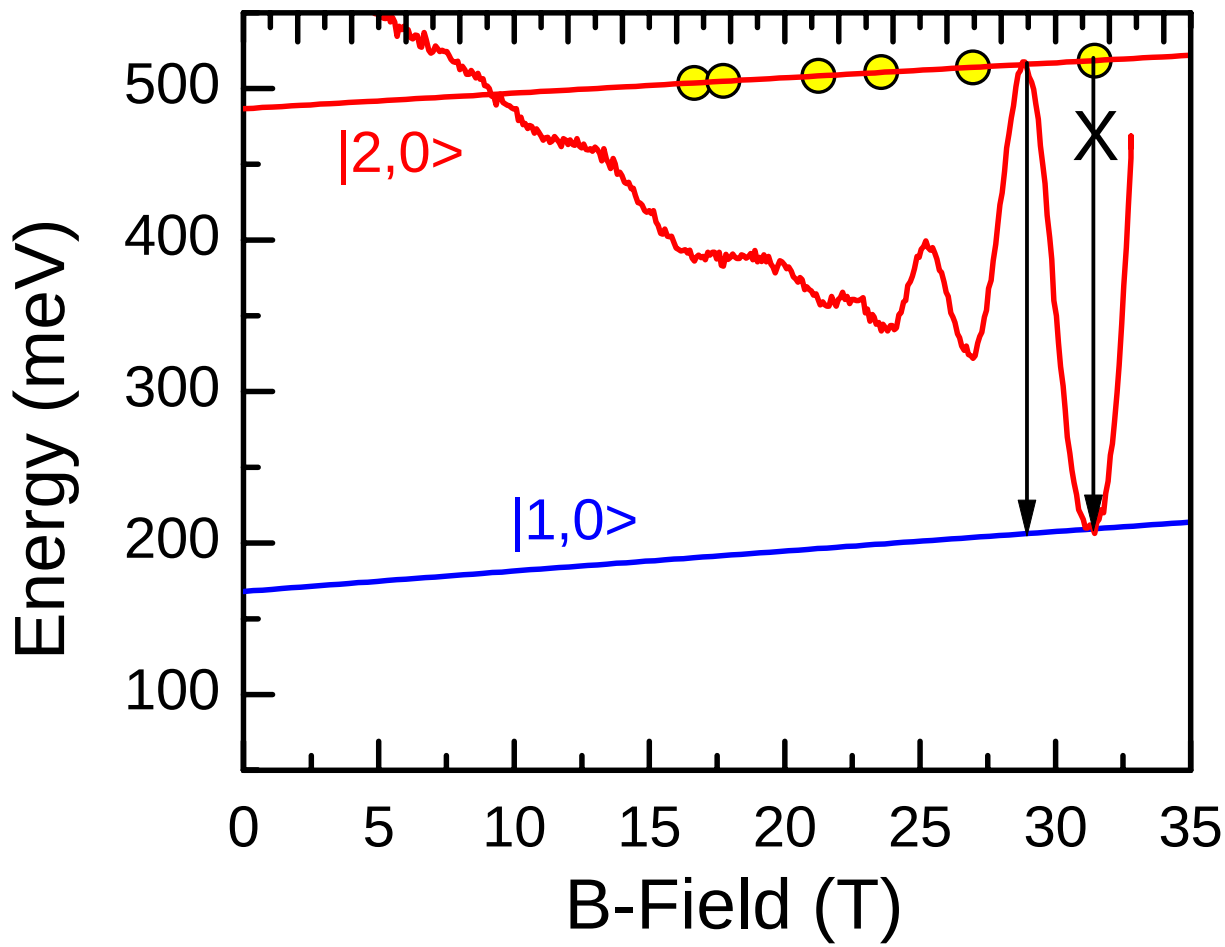

Scattering to the Landau Fan

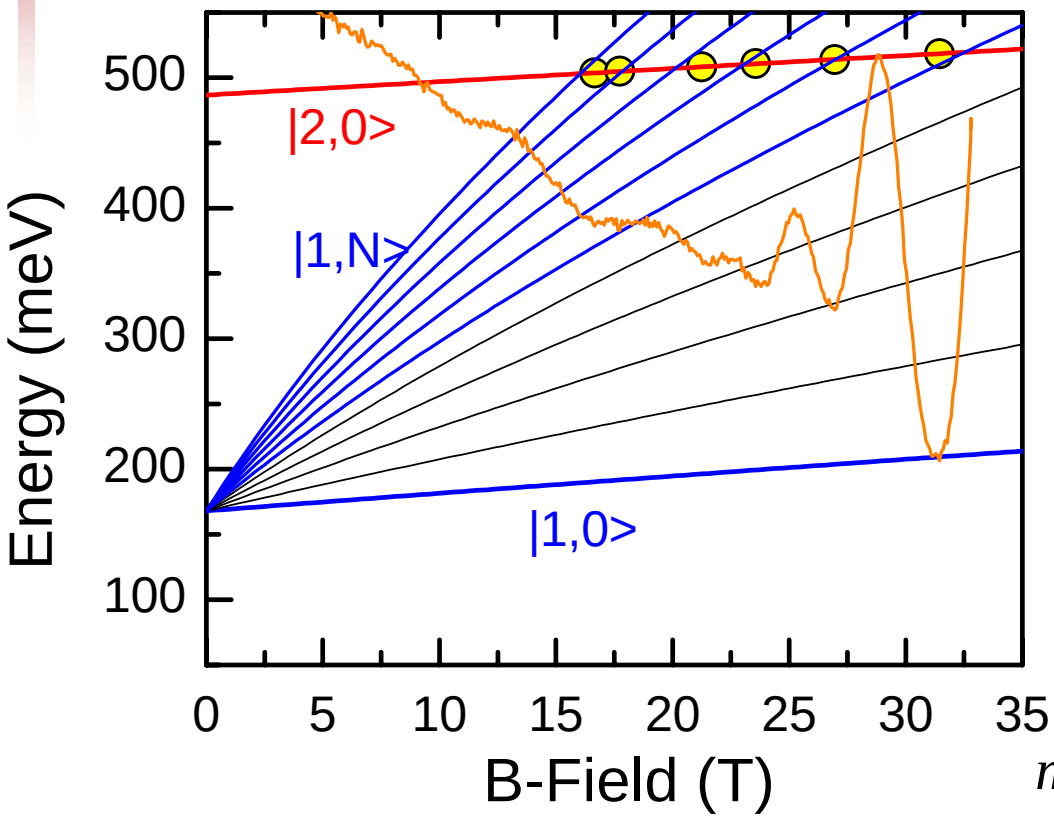

The emission intensity is smaller for resonances of Landau levels $|1,N>$ with the electrons in $|2,0>$.

Electrons scatter to lower laser state without emitting photon.

Feedback for $m^*(E)$

$$m^*(E) = m_0^* \left(1 + E / E_W\right)$$

Red shift with increasing B

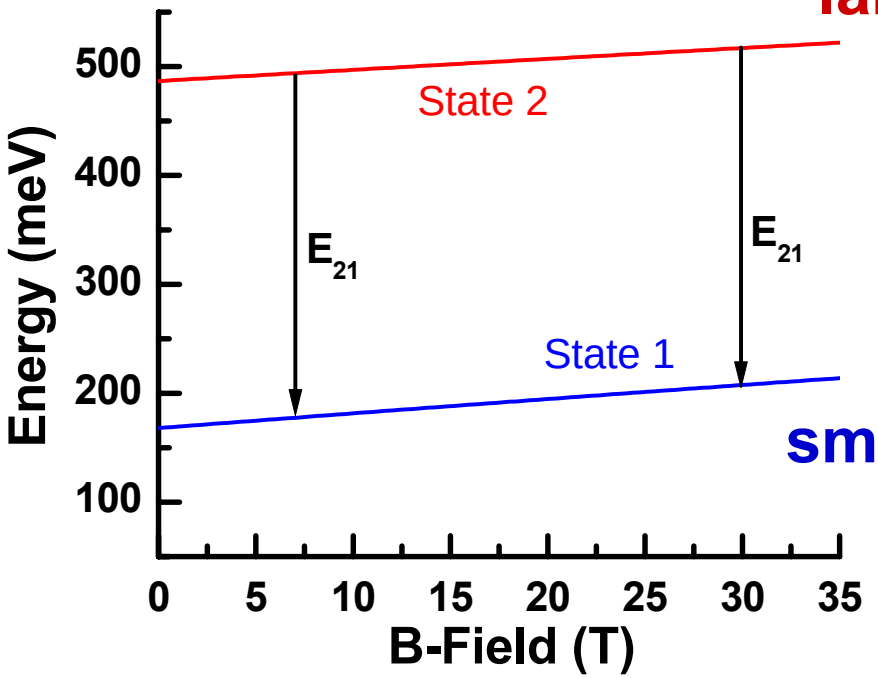

$$E_{i,0}(B) = E_i + \frac{\hbar e}{2m^*(E)} B$$

Thus, small red shift for E_2-E_1 with B.

$$\frac{dE_{21}}{dB} = -\frac{\hbar e}{2m_0}\left[\frac{m_0}{m_1^*} - \frac{m_0}{m_2^*}\right] \approx -5.95\mu_B \approx -0.35\,\text{meV/T}$$

Blue shift with increasing B

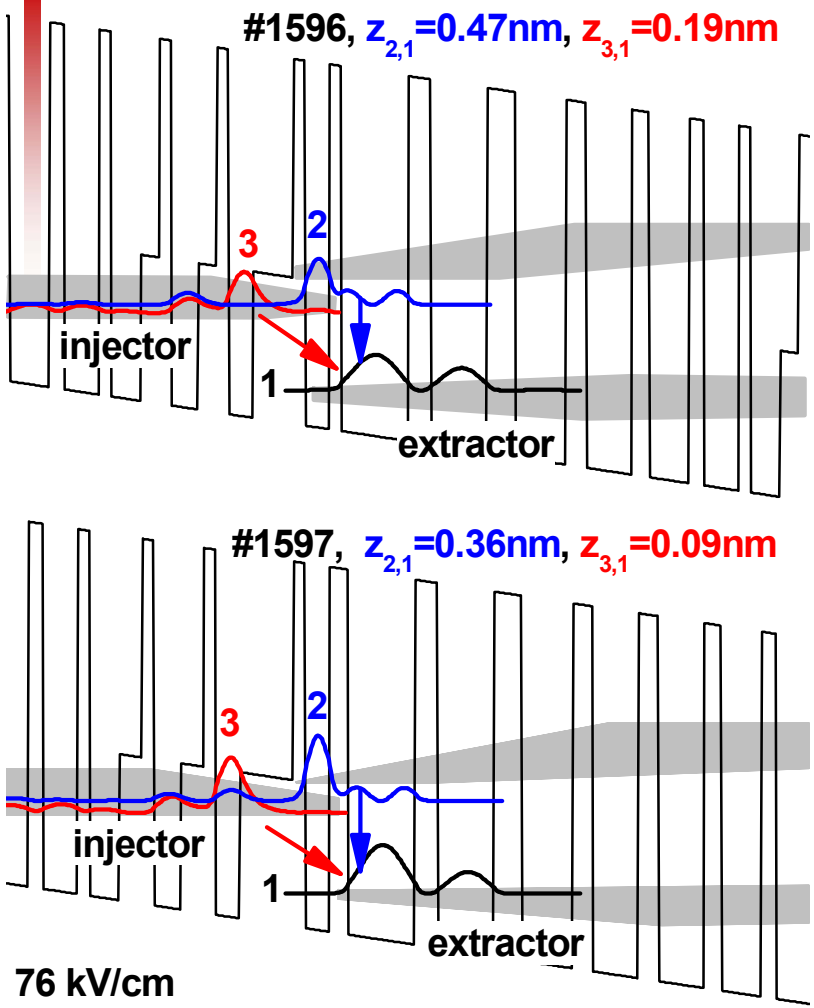

$$\frac{dE_{i1}}{dB} = e\frac{dU}{dB}\frac{(z_i - z_1)}{D_{tot}}$$

i=2 (**structure 1596**):

$$(z_2 - z_1) \approx 4.3\,\text{nm}$$

$$D_{tot} = 30 \times 47.8\,\text{nm} = 1434\,\text{nm}$$

$$\frac{\text{dU}}{\text{dB}} \approx 10\,\text{mV/T}$$

$$\frac{dE_{21}}{dB} \approx 0.03\,\text{meV/T} \approx 0$$

net red shift

Blue shift with increasing B

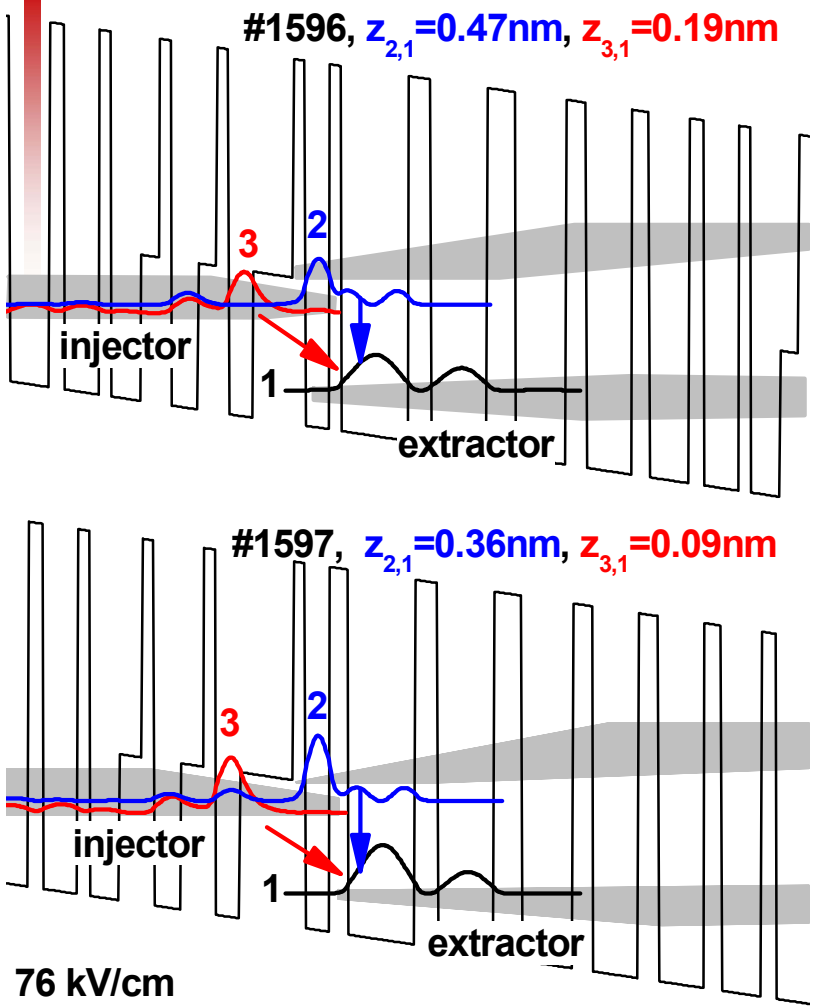

$$\frac{dE_{i1}}{dB} = e\frac{dU}{dB}\frac{(z_i - z_1)}{D_{tot}}$$

i=3 (**structure 1597**):

$$(z_2 - z_1) \approx 12\ \text{nm}$$

$$D_{tot} = 30 \times 54.8\ \text{nm} = 1644\ \text{nm}$$

$$\frac{\text{dU}}{\text{dB}} \approx 45\ \text{mV/T}$$

$$\frac{dE_{21}}{dB} \approx 0.3\ \text{meV/T}$$

Cancels red shift

Spectral Shifts with B

QCL 1596: Injector miniband strongly coupled to state 2, B has minimal effect on transport. ⇒ **Red Shift**

QCL 1597: Injector miniband weakly coupled to state 2, allows state 3 to invert and act as upper laser state, B has larger effect on transport.
⇒ **Zero or Blue Shift**

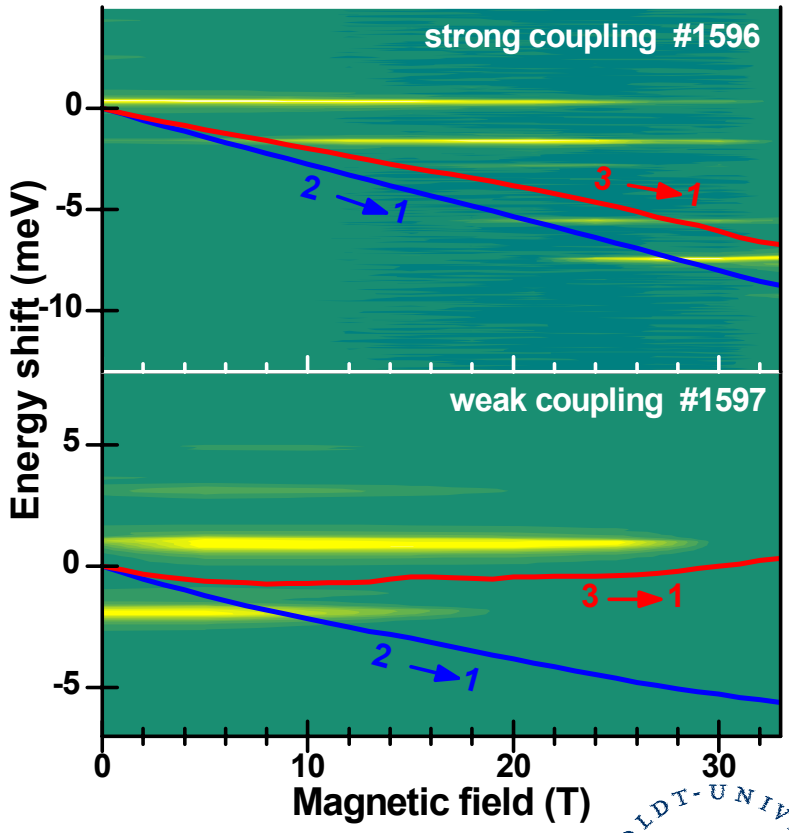

Lessons Learned

Increasing the barrier between the upper and lower states results in a more diagonal transition with higher threshold current.

Stark effect can help reach shorter wavelengths: Higher electric field, more diagonal transition.

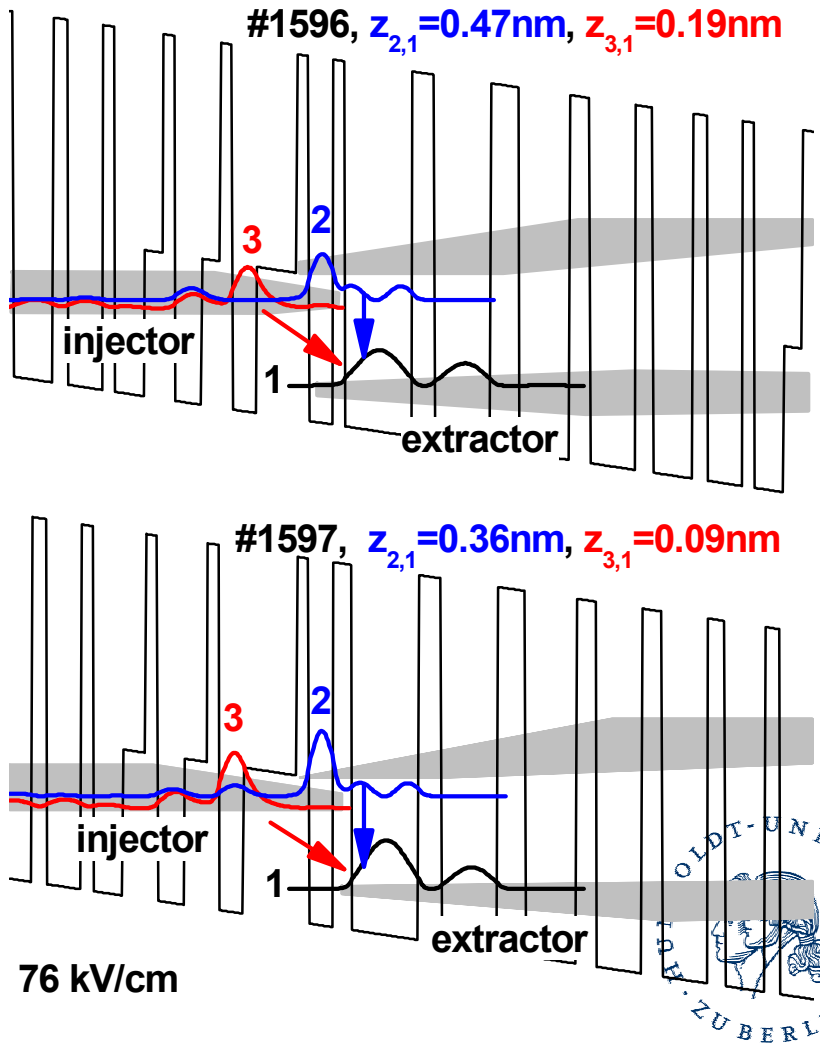

Location of upper laser level is important.

Three QCL designs emitting at 3.8 µm.

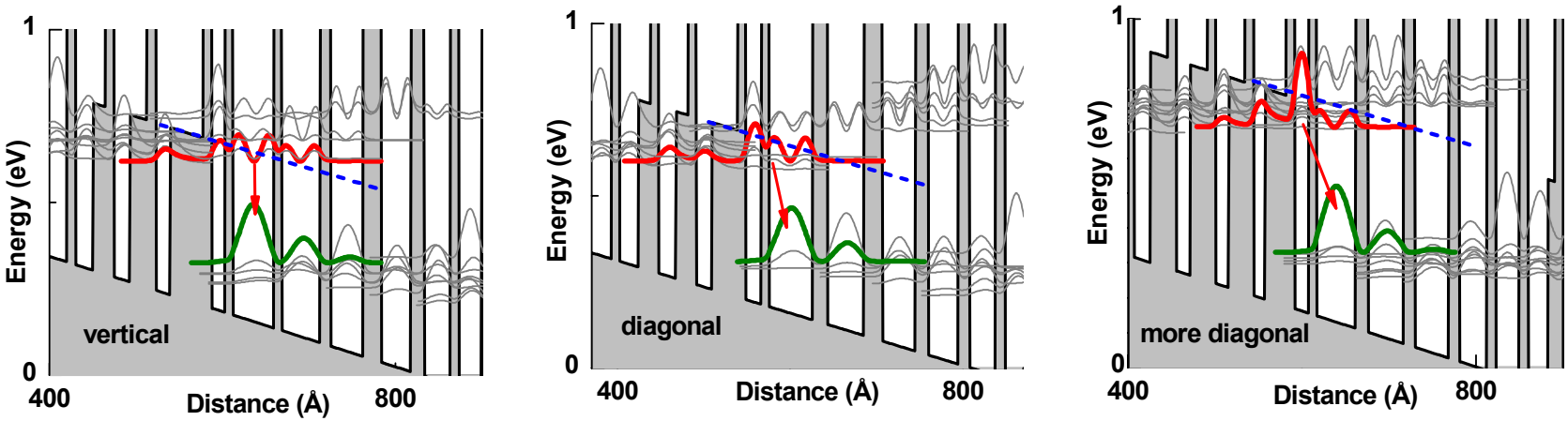

By varying the active region design, we can tune the location of the main upper laser level.

Experimentally we can determine it through the B-field dependence of the emission wavelength.

The location of the upper laser level influences the threshold and temperature dependence.

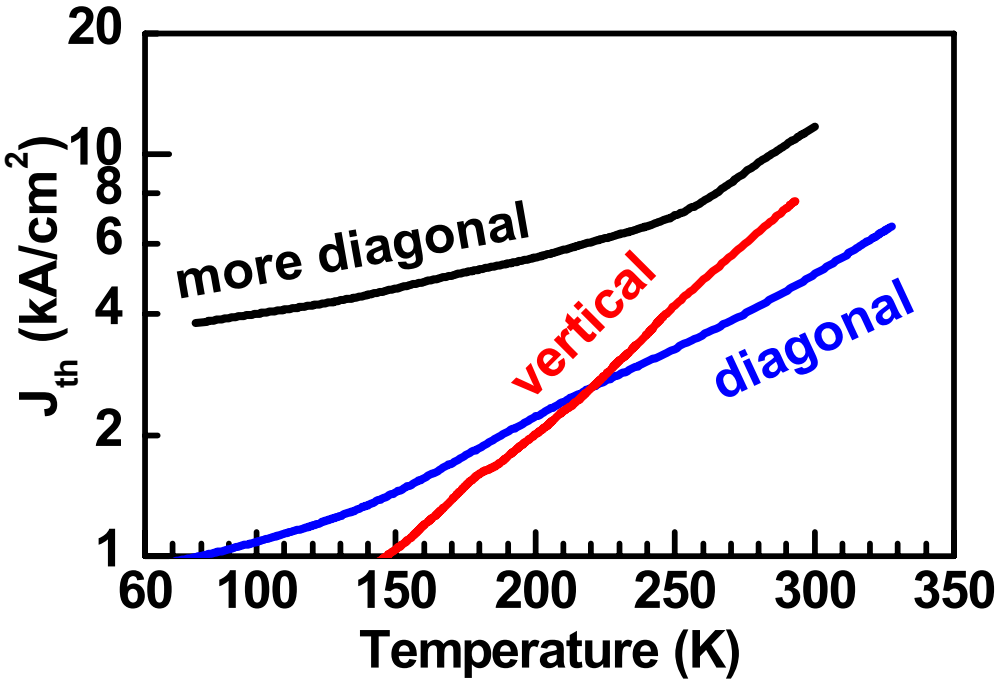

Upper states for diagonal transitions are less temperature sensitive, but do not couple as well to the lower laser state.

The “diagonal” design is pretty good and has a broad gain region.

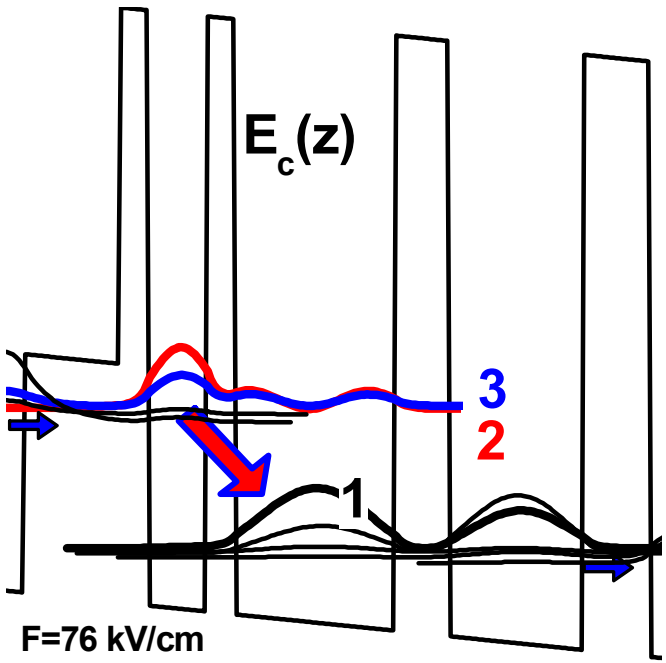

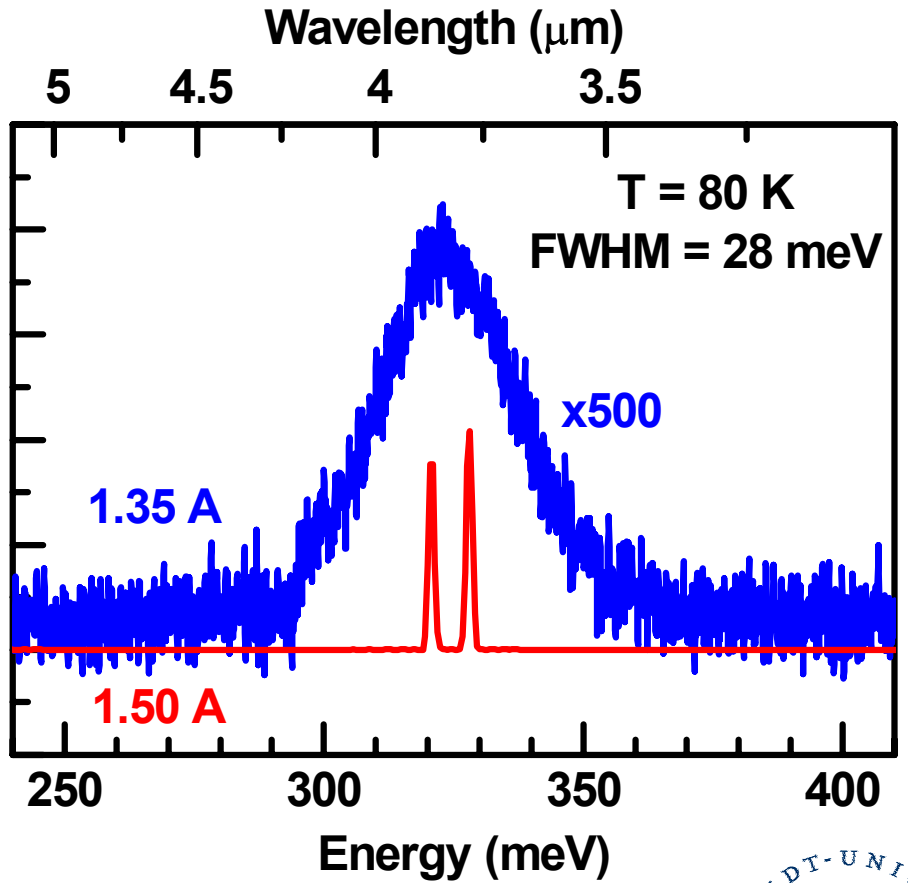

Thin injector barrier results in several ULLs and a broad gain spectrum.

External cavity tuning of broad-gain-region 3.8-µm QCLs

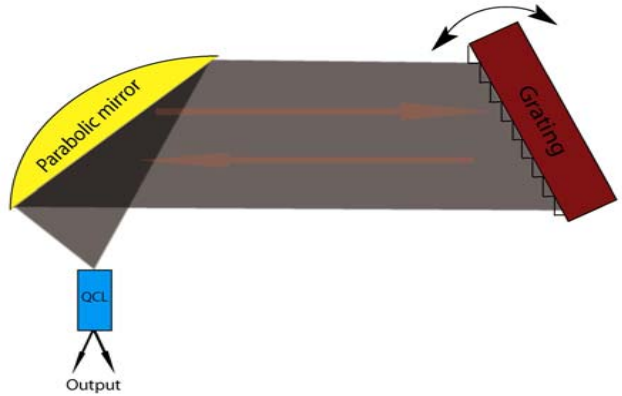

Without AR coating on facets.

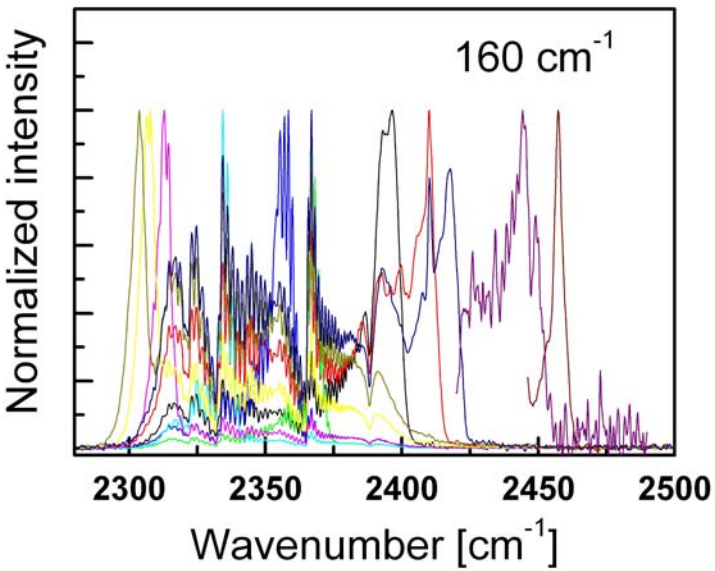

Littrow configuration using a parabolic mirror and a grating

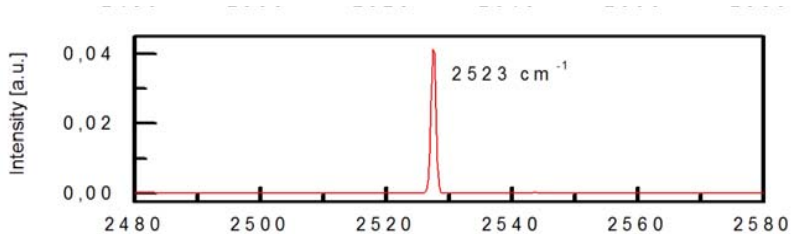

With AR coating on facet. (370 nm sputtered TiO_2)

We use similar designs for 3.6-μm QCL:

Our design works about as well at 3.6 μm as at 4 μm.

(6-μm × 5.5mm)

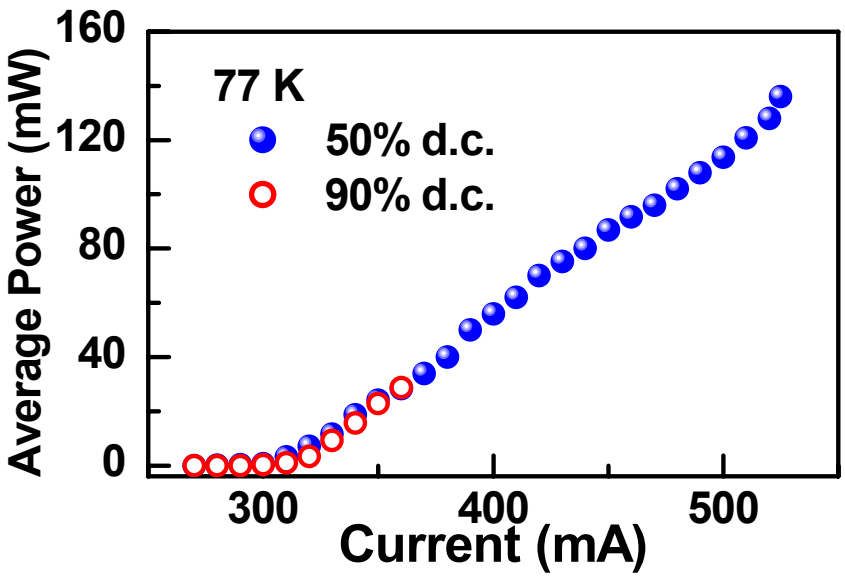

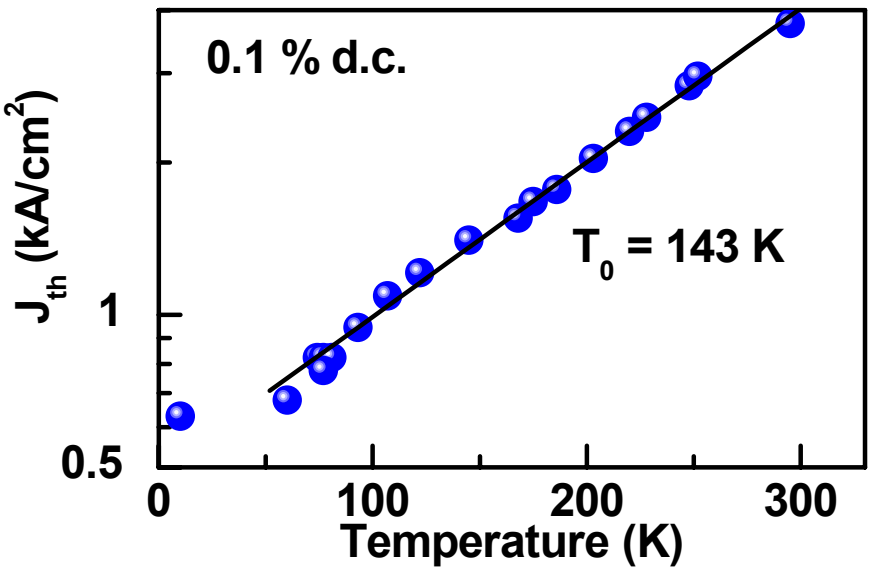

Total average power at 77K

Two major modifications to increase E_2-E_1:

1. Increase E_2 by locating it in AlInAs (not GaInAs) and at higher electric potential.

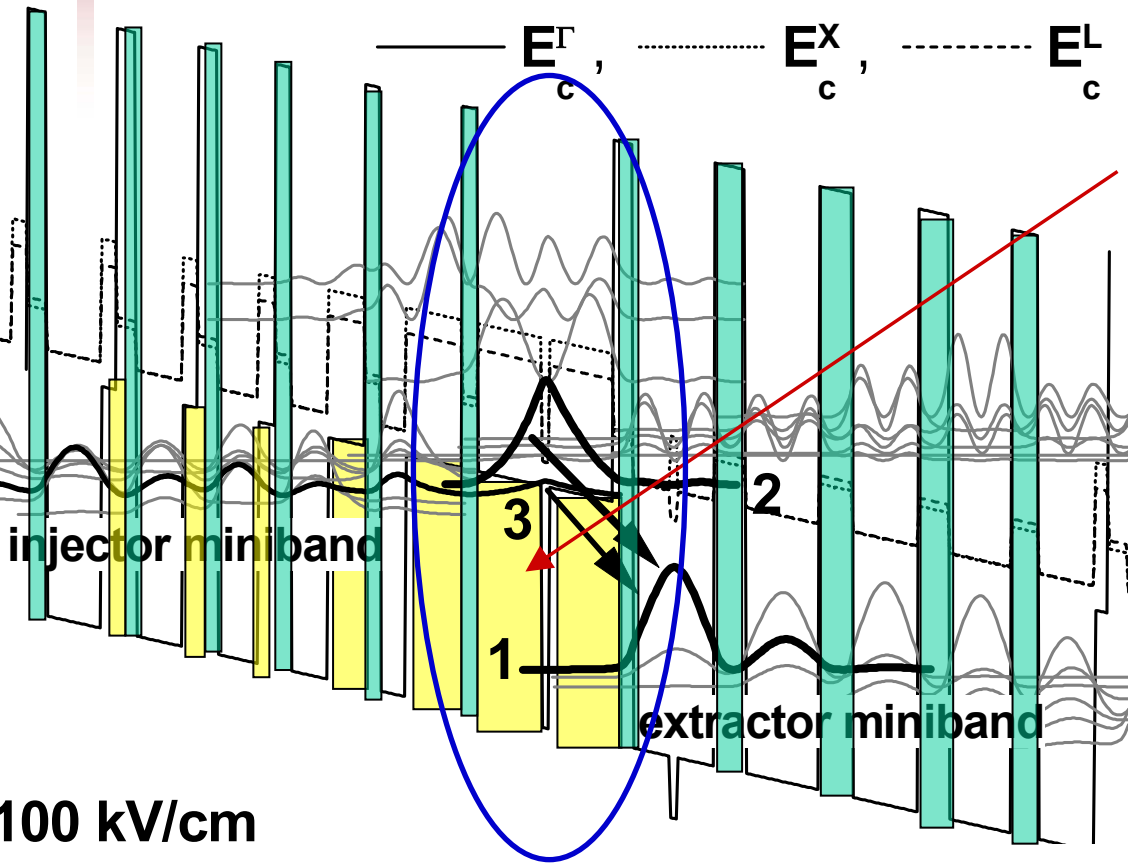

Upper laser states mostly located in AlInAs.

Upper laser states are high in energy and <u>not</u> well coupled to indirect valleys in lower QW.

Two major modifications to increase E_2-E_1:

2. Lower E_1 by adding thin InAs insert.

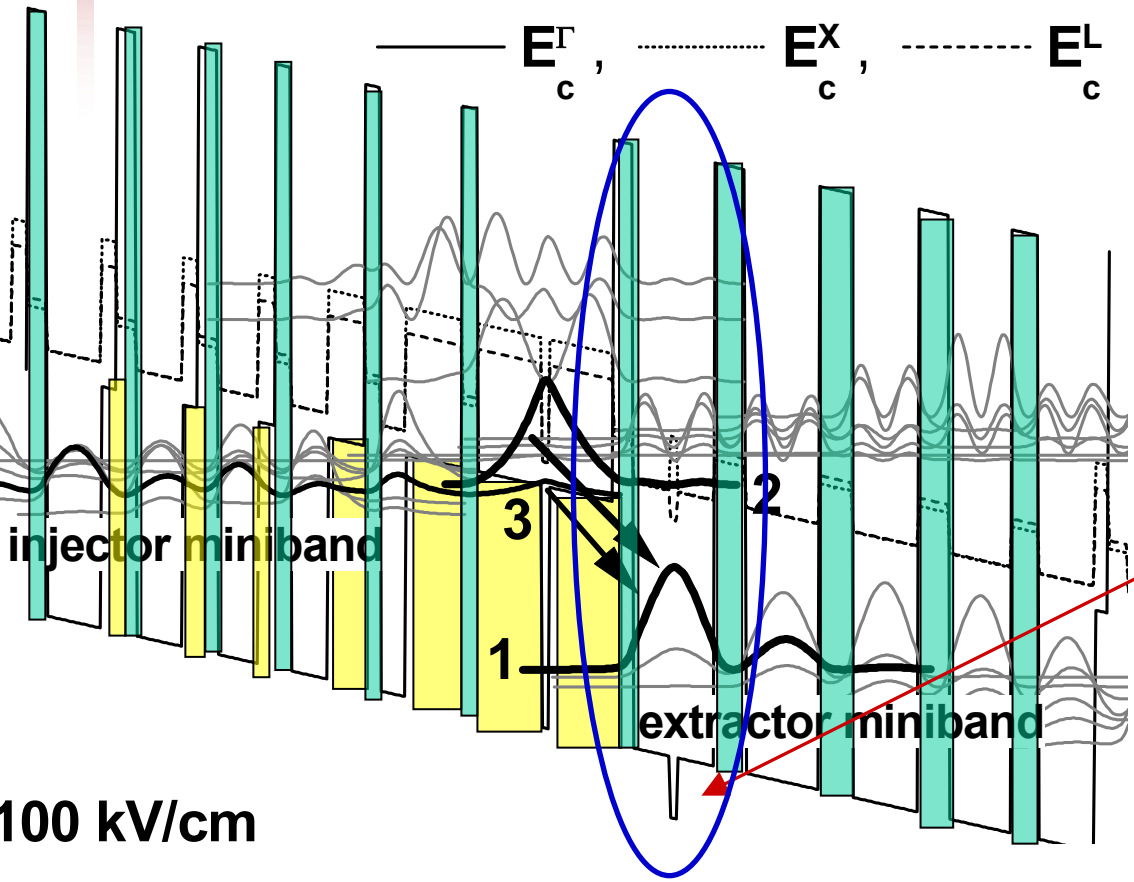

This design emits at 3.05 µm.

QW with lower laser state contains InAs insert.

The 3.05-μm QCL emits >100 mW power at 80K, but operates only up to 150K.

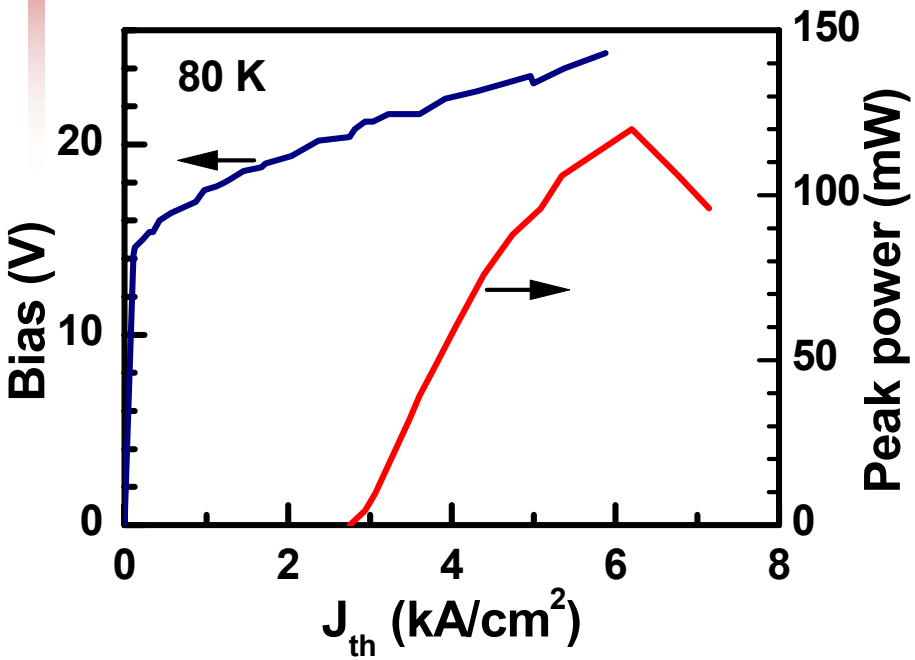

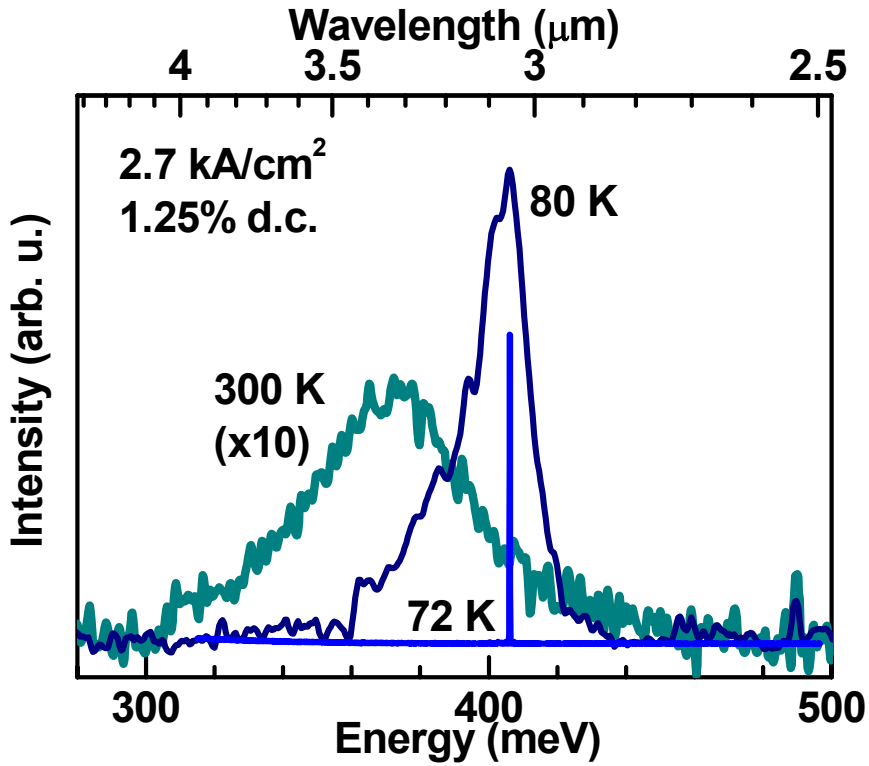

A similar design for 3.3 μm emits up to 600 mW and operates to 200K.

T_0 is high at low temperatures, in spite of indirect valleys.

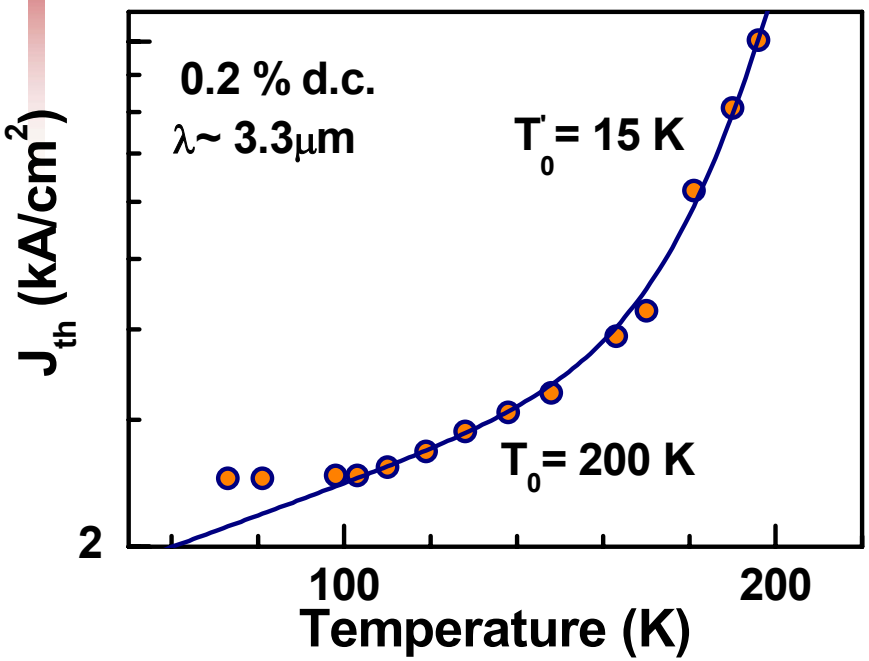

3.3-μm QCL

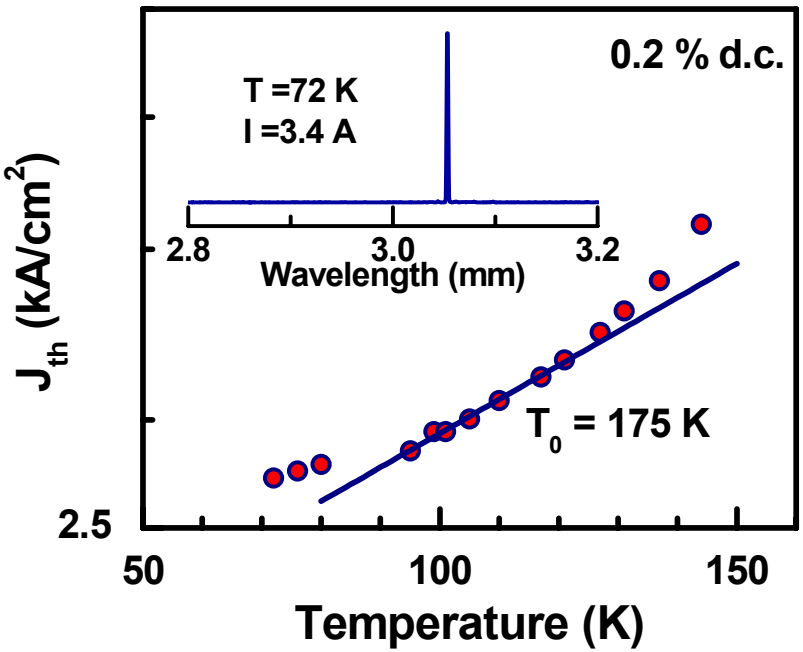

3-μm QCL

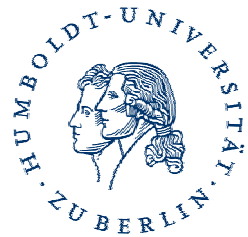

Short wavelength designs are limited by the indirect valleys.

Steep increase in J_{th} beginning at 150K is probably due to scattering into the indirect valleys.

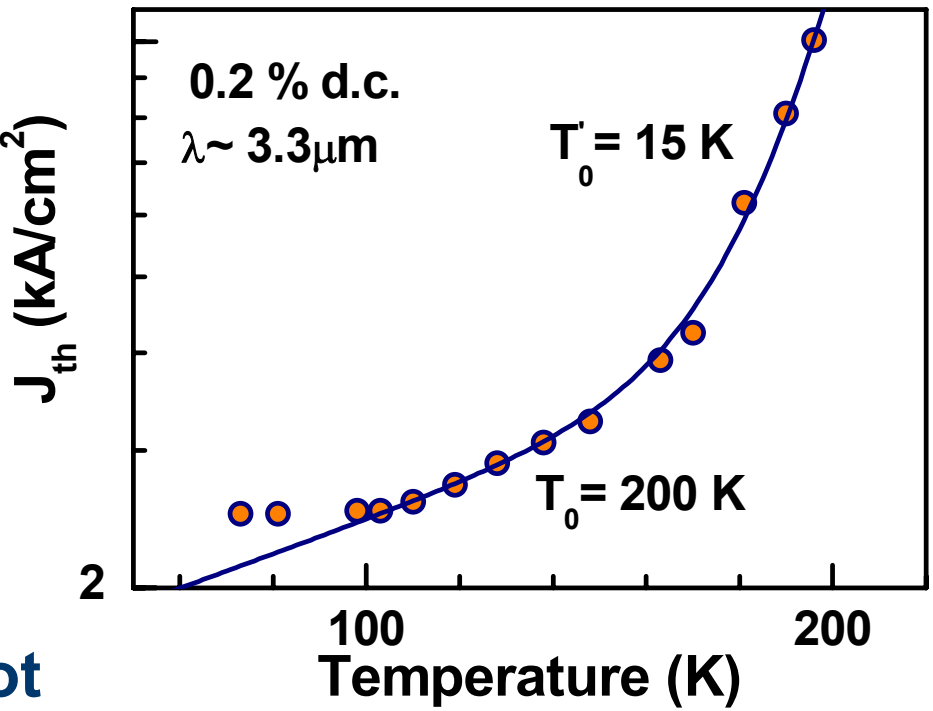

The indirect valleys do not prevent lasing, but still have adverse effects.

Question still remains: Where are the indirect valleys?

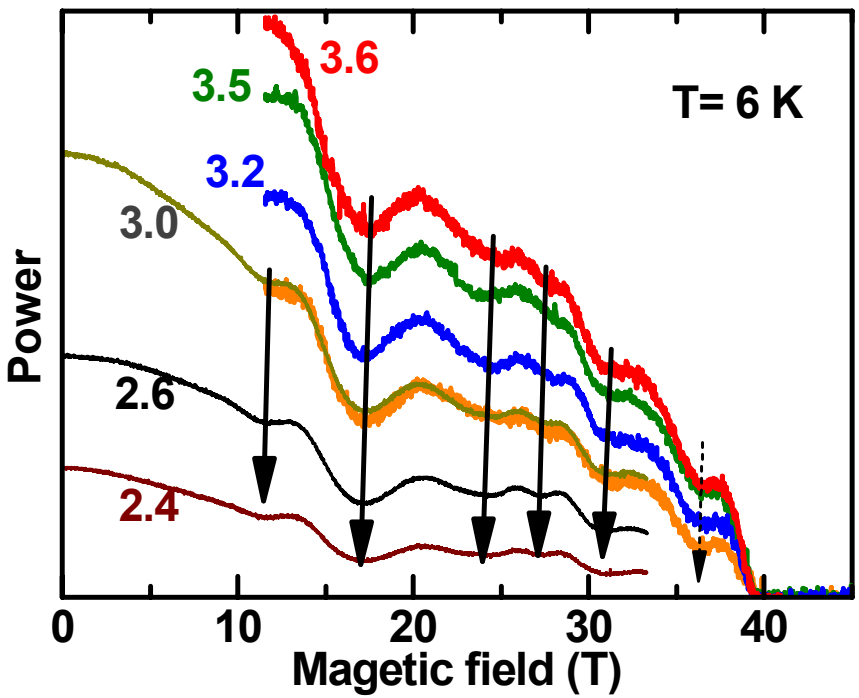

Output power from the 3.05-μm QCL oscillates in magnetic field.

Data measured at NHMFL, Tallahassee, with D. Smirnov and G. Federov

(Semtsiv, et al., APL 2008.)

Minima in oscillations due to non-radiative scattering from E_2 into Landau levels of E_1

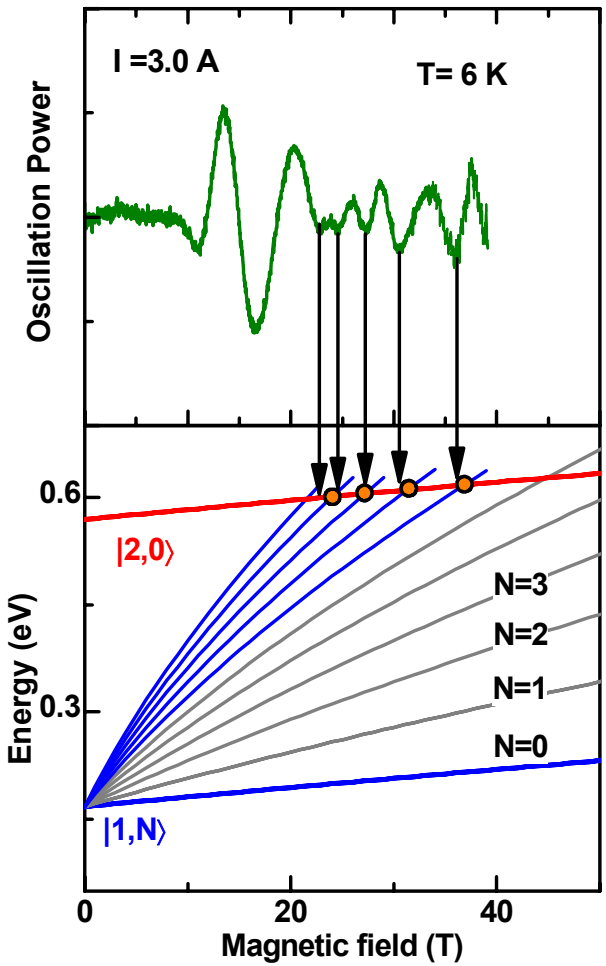

Electrons in |2,0⟩ scatter into Landau levels of lower laser level:

- No phonon involved; momentum taken care of by interfaces.
- Landau levels 6, 7, 8, 9; weaker as ΔN is larger.
- Laser is turned off by fields B>40T so N<6 not seen.
- Extra oscillations (strong) between 10 and 20 T.

New oscillations due to electrons in excited Landau levels of E_2 scattering into X valley

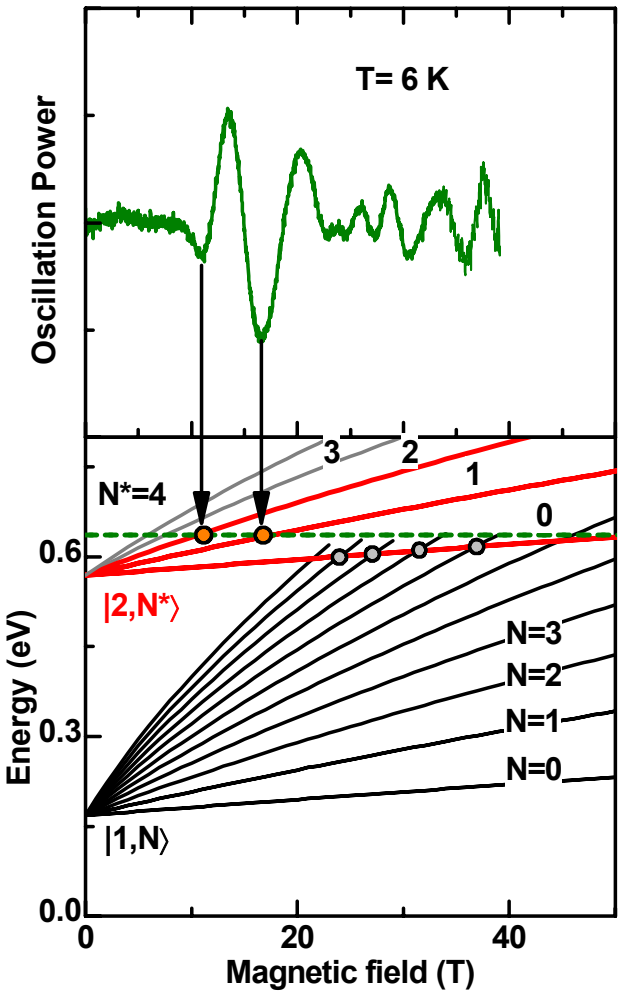

- Landau levels for E_2 with N>0 should be thermally occupied.
- Proposed resonant energy level is independent of B ⇒ heavy m*.
  - Level is about 70 meV above E_2 at B=0.
  - Likely to be $X_{x,y}$ valleys shifted lower due to uniaxial component of strain.

When the lowest Landau level is nearly in resonance, the laser shuts off.

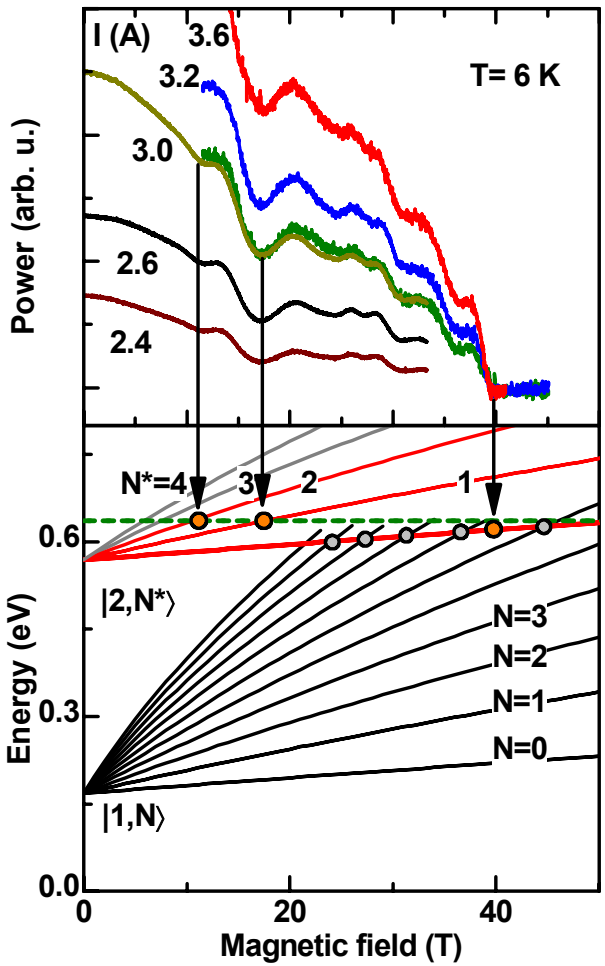

We propose that when the N=0 Landau level is nearly resonant with the indirect valleys, lasing is no longer sustainable.

If the lowest indirect valley is 70 meV above the upper laser level, it is 470 meV above the lower laser level, and about 640 meV above the Γ level.

This value is about 40 meV higher than expected from our model.

Both the maximum temperature of operation and the onset of low T_0 decrease with emission wavelength.

The trend of steadily decreasing temperature for the onset of low T_0, despite many changes to the active region, implies that the culprit is the indirect valleys.

Extrapolating these results implies an ultimate limit of about 2.7 μm.

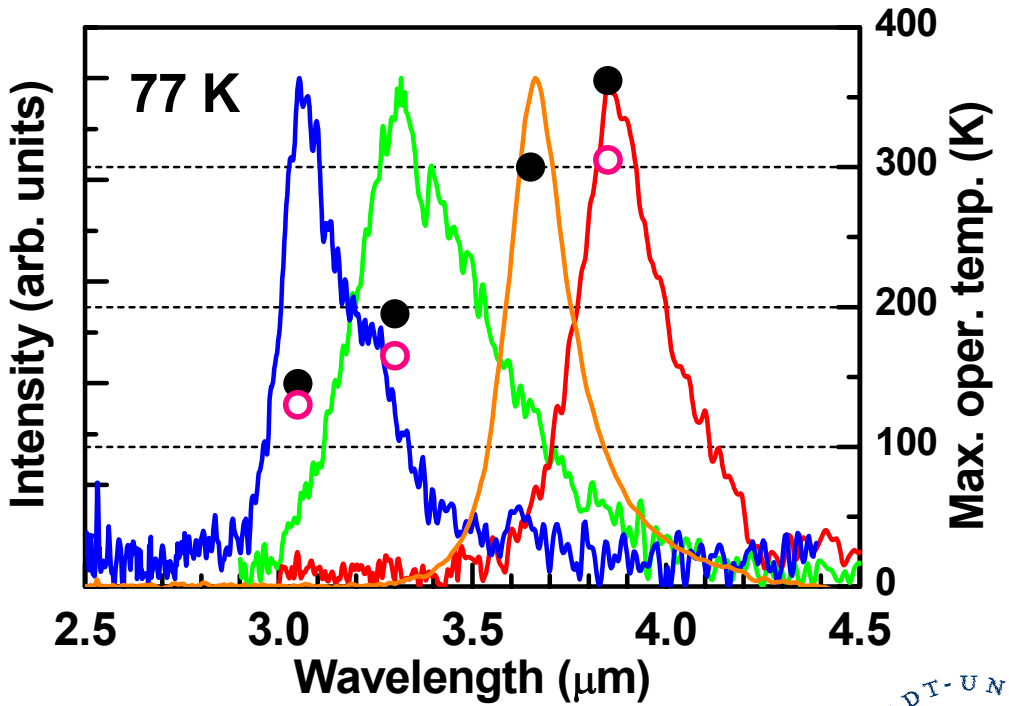

Laser Power and Efficiency in Pulsed Mode (old 3.8-μm data)

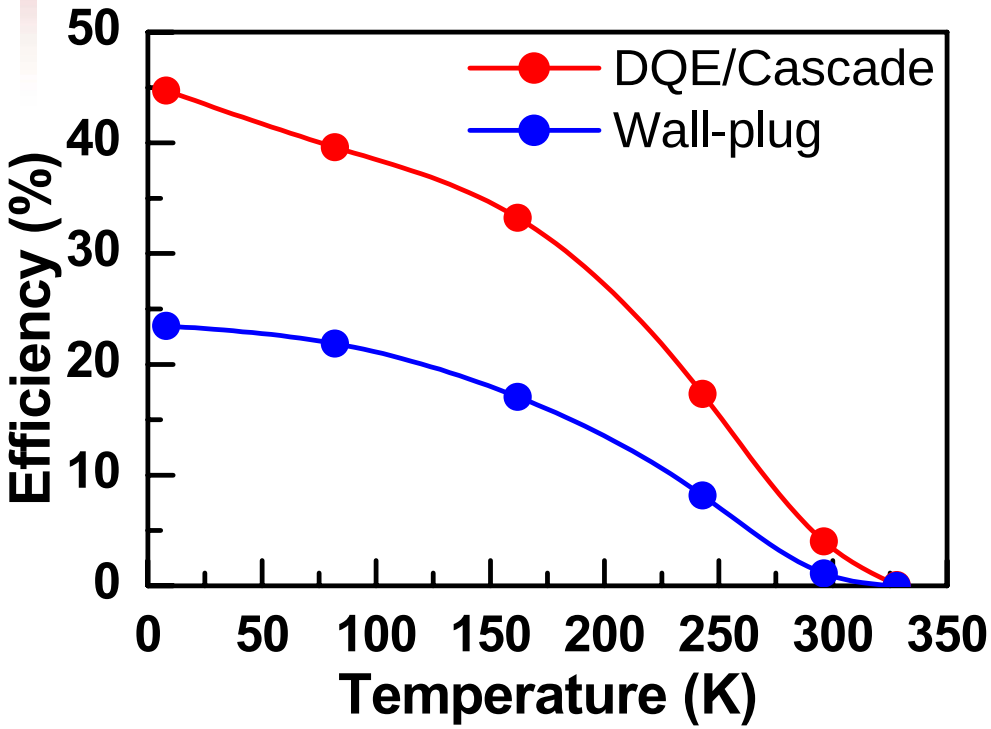

8 K:

- Maximum power 12 W
- Total DQE of 1300%
- DQE/cascade of 45%
- Power efficiency 23%

243 K (-30˚C):

- Maximum power 4 W @5 A, 10 V

300 K:

- Maximum power 0.45 W @4 A, 10 V

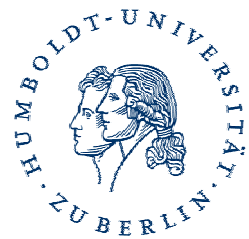

Really high performance at 3.8 μm requires a number of processing improvements.

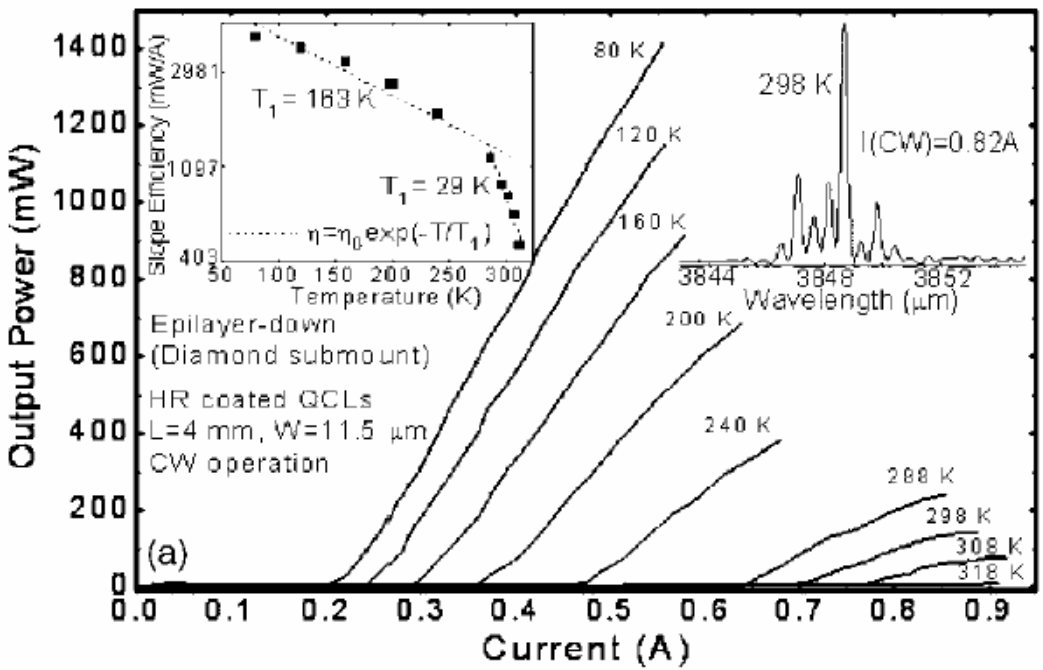

Razeghi Group 2008

1.4 W at 80 K

See Manijeh Razeghi invited talk Thursday.

More recently our focus is on improving the beam quality by using narrow ridges.

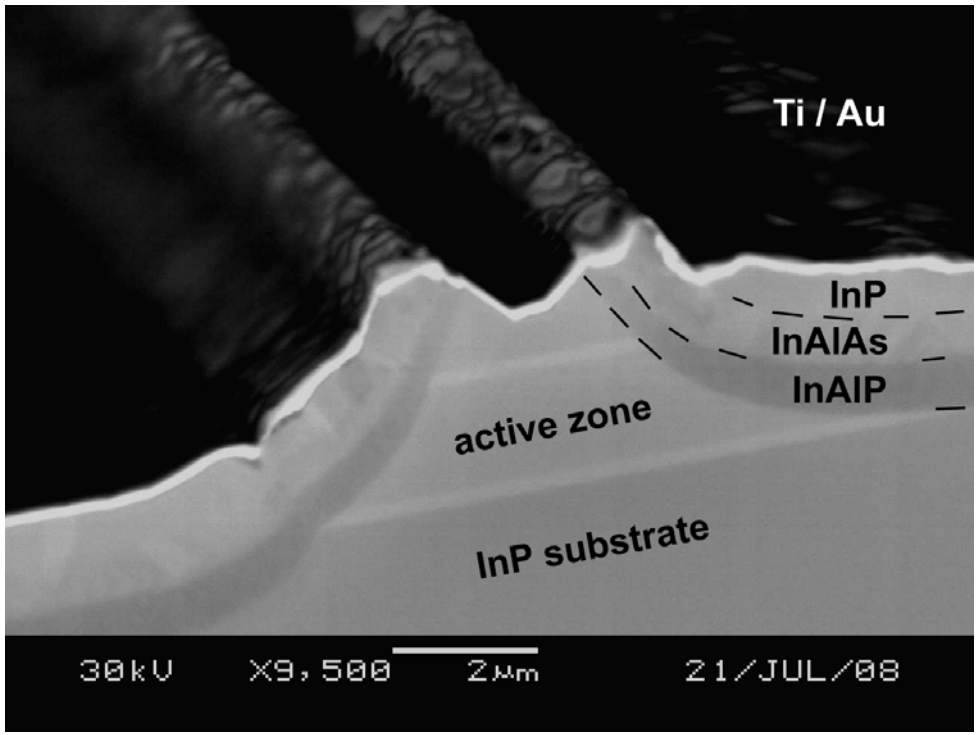

The ridge is wet etched to about 5 µm and overgrown with InAlP, InAlAs, InP.

A 5-μm ridge has similar lateral and transverse apertures and emits a nearly circular beam.

The beam is nearly circular with a divergence of 46°.

The beam quality factor $M^2 \approx 1.6 \Rightarrow$ well-suited for spectroscopy and imaging.

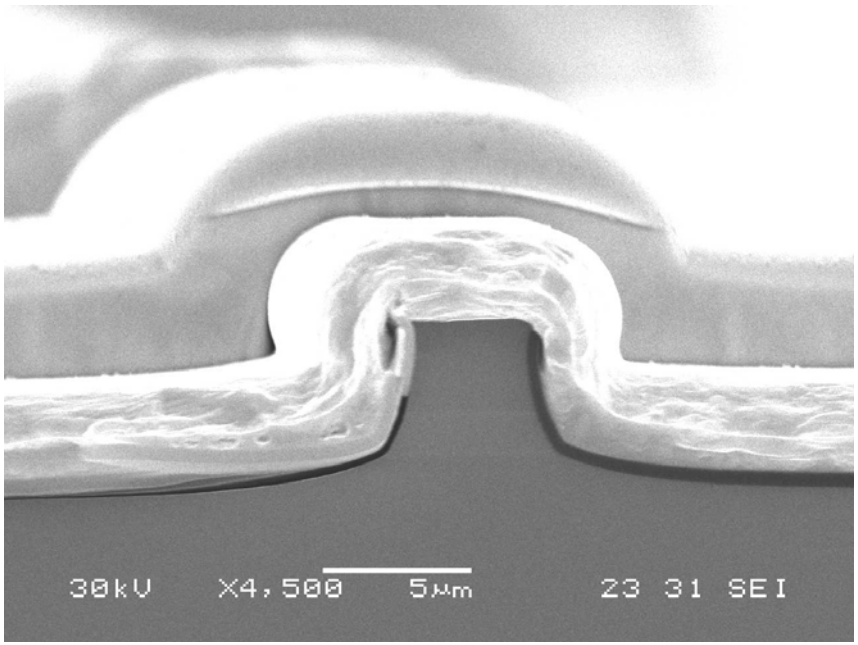

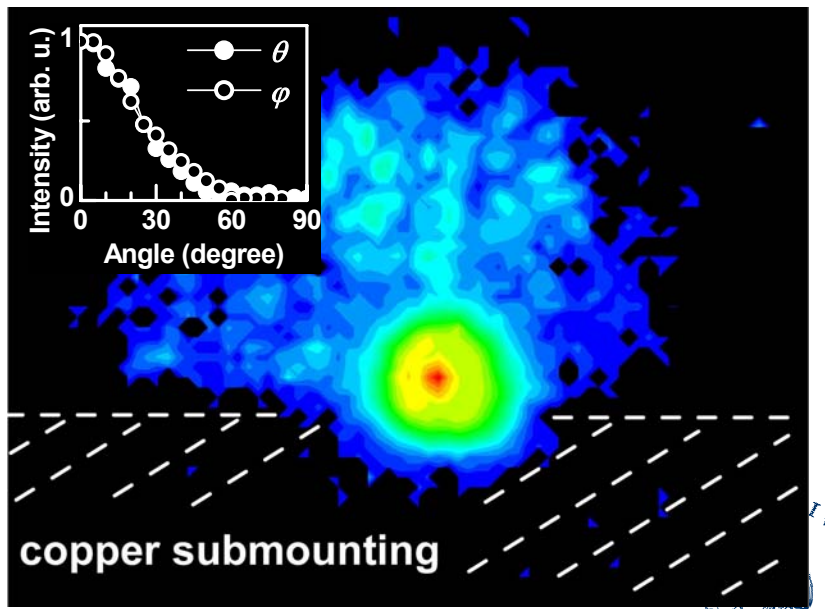

with K. Kennedy and R. Hogg, University of Sheffield

High power from narrow ridges:

Average power of 200 mW with 50% duty cycle.
Slope efficiency = 0.42 W/A

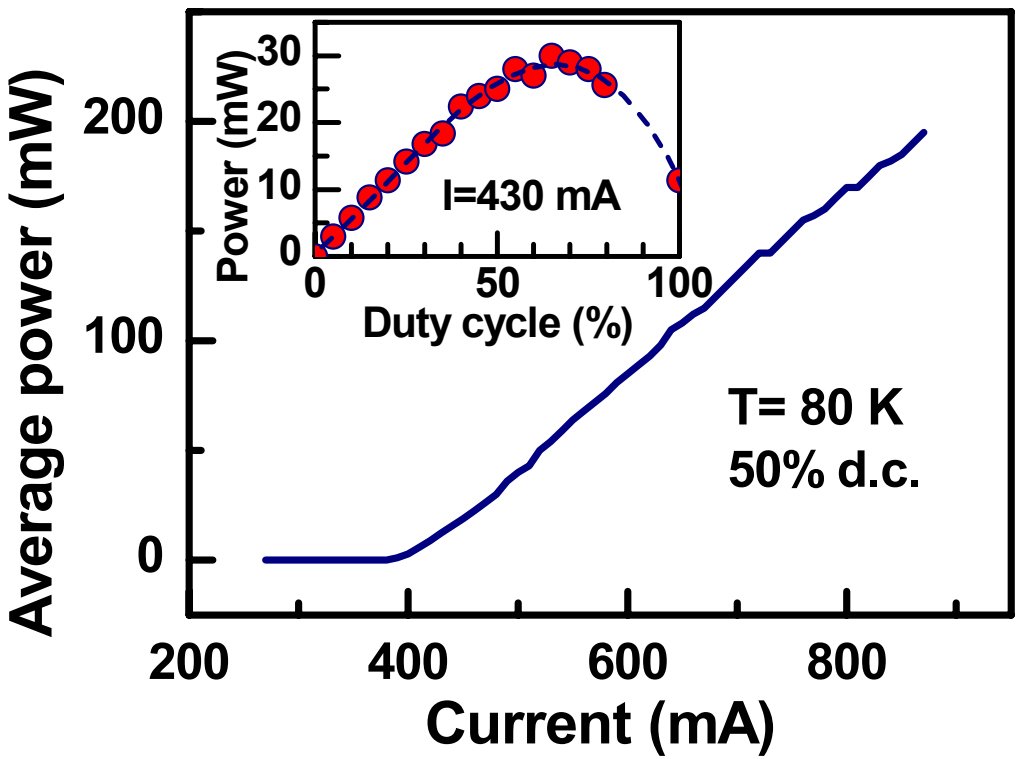

with K. Kennedy and R. Hogg, University of Sheffield

Humboldt-University Peltier-cooled housings reach temperatures of -40°C.

Despite the narrow ridge, power levels are quite high at Peltier temperatures.

We obtain peak power of 450 mW and average power of 60 mW at 3.9 µm.

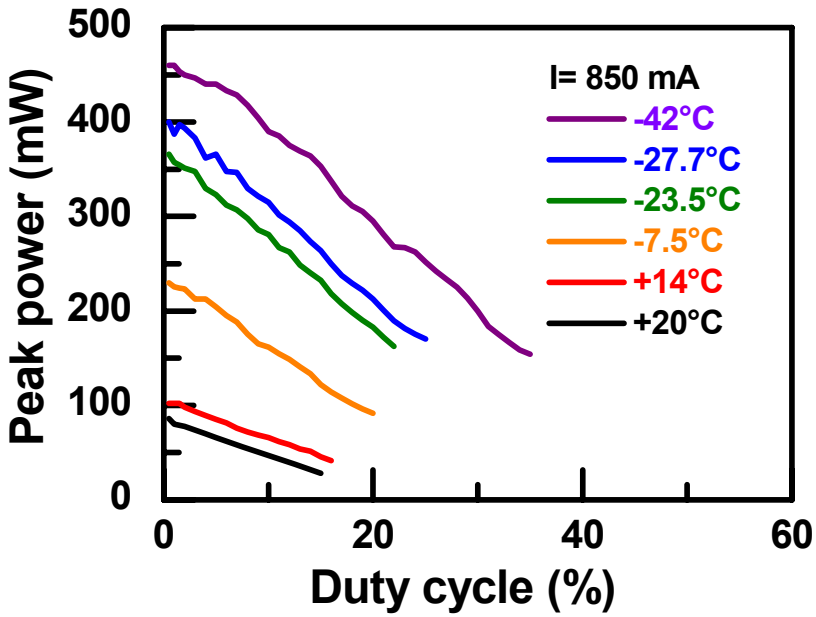

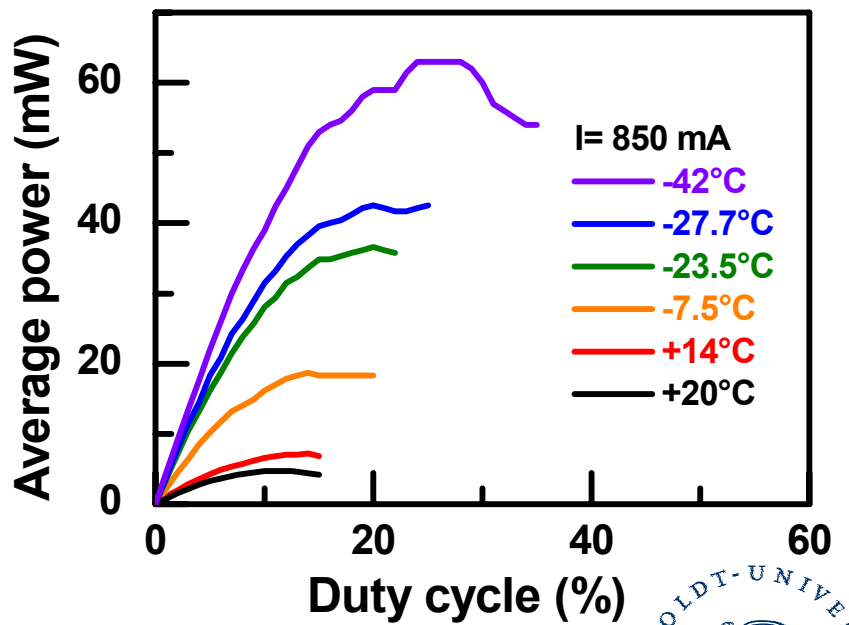

with K. Kennedy and R. Hogg, University of Sheffield

Surface-emitting (4 µm) QCL ring lasers

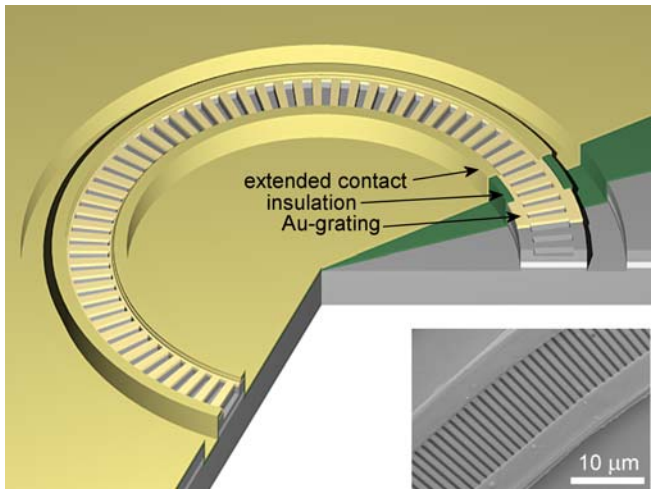

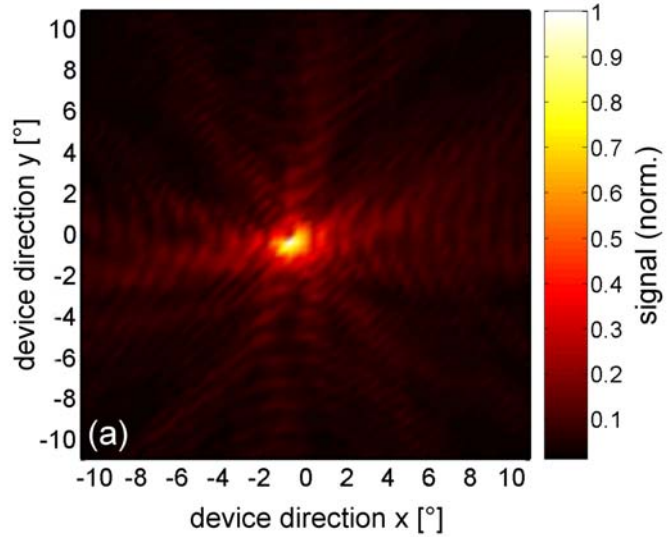

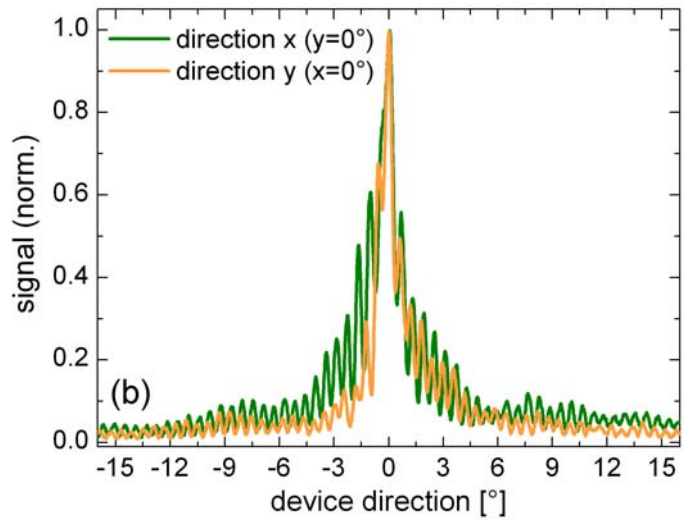

Elvis Mujagić, et al. (TU Wien + HU Berlin)
(Poster on Thursday)

Summary

- Strain compensation extends the useful range of QCLs based on InP. (Demonstrated to 3.05 µm. Possible 2.7 µm?)
- 1st atmospheric window covered
- For large enough ΔE_c , it is the indirect valleys of the well material that limit emission wave length.
- New design features to avoid emptying upper laser state into InGaAs indirect valleys. (Diagonal transitions, “barrier material” for ULL, InAs for LLL.)
- Narrow ridges for excellent beam quality

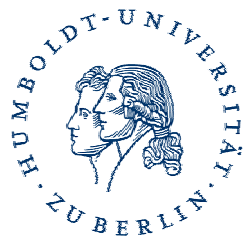

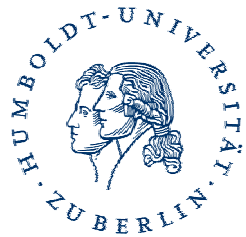
HUMBOLDT-UNIVERSITÄT ZU BERLIN